Journal of Transport Geography 133 (2026) 104611

Contents lists available at ScienceDirect

Journal of Transport Geography

journal homepage: www.elsevier.com/locate/jtrangeo

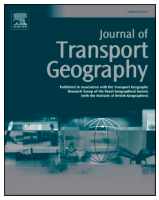

An optimization framework for the design and operation of efficient urban air mobility systems: An application in the Île-de-France region

Sam Randeraad [a,*], Marta Ribeiro [a], Jan Anne Annema [b], Gonçalo Homem de Almeida Correia [c]

[a] Department of Control & Operations, Faculty of Aerospace Engineering, Delft University of Technology, Delft, the Netherlands
[b] Department of Engineering Systems and Services, Faculty of Policy and Management, Delft University of Technology, Delft, the Netherlands
[c] Department of Transport & Planning, Faculty of Civil Engineering and Geosciences, Delft University of Technology, Delft, the Netherlands

ARTICLE INFO

Keywords:
Urban air mobility
Vertiport placement
Fleet-size optimization
Multi-objective optimization
Demand-supply interaction

ABSTRACT

Urban Air Mobility (UAM) systems offer a three-dimensional transportation alternative by using low-altitude airspace, with the potential to reduce travel times and improve access to mobility in regions underserved by current transportation systems. To support efficient design and operation of UAM systems, we develop an integrated optimization framework in response to three interrelated challenges: (i) land use, aeronautical feasibility, community acceptance and other factors that restrict the number of potential locations for vertiports, (ii) bidirectional demand–supply interaction that needs to be considered, as the level of service influences demand for UAM and operators adjust the level of service in response to demand, and (iii) strong interactions between strategic decisions on the distribution of ground infrastructure, tactical decisions on eVTOL fleet size and operational decisions on dispatching and repositioning. Analyzing the decisions in isolation can lead to poor estimates of the overall system performance. The framework consists of (1) a knock-off criteria analysis model for the identification of a realistic set of candidate locations for vertiports, (2) integer programming models in which strategic, tactical and operational decision levels are modeled, and (3) pre-processing techniques to generate near-optimal solutions for real-world instances. By applying the framework in a large-scale real-world setting in the Île-de-France region, we demonstrate complex interactions between strategic, tactical, and operational decision levels and customer demand, revealing various trade-offs between operator profit and traveler generalized travel costs.

1. Introduction

Major urban areas are struggling to meet the growing travel demand with their current ground transportation systems. Rapid population growth, urbanization, and the rise in privately-owned vehicles have led to widespread traffic congestion, resulting in economic losses and environmental pollution. On the positive side, urban transportation is undergoing rapid transformation due to new on-demand services (e.g., ride- and car-sharing) and advanced technologies (e.g., electric and autonomous vehicles). However, achieving long-term sustainable urban transportation may necessitate the introduction of additional disruptive technologies and innovative business models.

The increasing pressure on the ground transportation systems, together with limited space for expansion, pushes urban transportation into the third dimension: the sky. Due to recent advancements in electric propulsion, what was once a science fiction topic is currently becoming a reality: electric Vertical Takeoff and Landing vehicles (eVTOL) (Garrow et al., 2021; Staubinger et al., 2020). As of early 2024, over 500 eVTOL designs have been proposed, with multiple designs close to regulatory certification. Manufacturers claim that eVTOLs can support short-range services with small payloads (i.e., a few passengers) at lower operating costs and with a reduced acoustic footprint compared with conventional helicopters (EvE, 2022). Nevertheless, concerns remain regarding the effects eVTOL operations may have on local communities, particularly in dense urban environments (Pons-Prats et al., 2022).

The development of eVTOLs has given rise to the concept of Urban Air Mobility (UAM) in transportation. UAM has the potential to provide an alternative three-dimensional mode of passenger transport by utilizing low-altitude airspace. Cities and operators are already making significant investments in UAM. For example, cities such as Paris, Dubai, Singapore, and New York are partnering with manufacturers to accelerate UAM development (SMG Consulting, 2025). Additionally, various

* Corresponding author.
E-mail address: s.j.randeraad-1@tudelft.nl (S. Randeraad).

https://doi.org/10.1016/j.jtrangeo.2026.104611
Received 10 September 2025; Received in revised form 18 January 2026; Accepted 21 February 2026
Available online 21 March 2026

airlines have ordered eVTOLs to offer airport shuttle services and regional flights (Archer Aviation, 2025). In this paper, we focus on the passenger air taxi use case within UAM and do not consider other UAM applications such as cargo transport or emergency services.

The characteristics of UAM systems make them quite different from existing technologies in air and ground transportation (Garrow et al., 2021). Compared to airlines with scheduled large-capacity flights, air taxi involves reservation-based, on-demand operations with a small payload. In contrast to ride-sharing services that utilize free-floating operations, UAM relies on dedicated infrastructure known as *vertiports*. Vertiports serve as designated locations from which eVTOL aircraft can take off and land, embark and disembark passengers, and recharge. The attractiveness of such UAM systems is determined by the level of service offered and the cost associated with using the system. The level of service is influenced by the accessibility of vertiports by potential travelers, i.e., (i) the access and egress time from the origin and destination to the vertiports, and (ii) the availability of eVTOLs at the vertiports. On the other side, the number and size of vertiports, the fleet size, and availability of eVTOLs at the "right" time and location influence the cost of establishing and operating a UAM system.

Planning UAM systems is complex due to several factors. First, eVTOL takeoff and landing are restricted by land use, aeronautical feasibility, accessibility, and community acceptance, limiting potential vertiport locations and necessitating integration with other transport modes (Wu and Zhang, 2021; Pons-Prats et al., 2022; Schweiger and Preis, 2022). Second, the on-demand nature and one-way demand patterns (e.g., city center peaks) may cause eVTOLs to accumulate at certain vertiports and be scarce at others. Relocation of empty eVTOLs can mitigate this, similar to car-sharing systems, preventing unnecessary fleet size increases and underutilization (Boyaci et al., 2015). Third, there are interdependencies between UAM operations and passenger demand; faster UAM trips tend to induce higher demand (Wu and Zhang, 2021).

For the effective and cost-efficient planning of UAM systems, models are required that decide on strategic decisions on vertiport location, size and number, tactical decisions on fleet size and operational decisions spanning eVTOL routing, repositioning and charging, while capturing the interaction of these decisions with passenger demand. The models should assist decision-makers in finding an optimum balance between the level of service offered and the total cost for implementing and operating the UAM system. However, the literature currently lacks modelling approaches that simultaneously consider the interdependencies between strategic vertiport planning, tactical fleet size planning and eVTOL operations. Existing models tend to look at the planning problem either solely from a strategic or tactical/operational perspective. Studies on strategic design of the UAM infrastructure network (Wu and Zhang, 2021; Rath and Chow, 2022; Boo et al., 2023) consider the interaction with customer demand but neglect the interaction with fleet operations. Tactical/operational studies (Rajendran and Shulman, 2020; Husemann et al., 2023; Li et al., 2020) mostly focus on finding the optimal fleet size and dispatching logic, tracking each eVTOL's activities independently. These studies take the UAM infrastructure network either as given or vary it through post-processing and sensitivity analysis. At last, in most studies, the set of potential locations for vertiports is either given or based on what could be ideal locations given spatial demand and existing heliports. In reality, there are restrictive requirements and other relevant criteria that need to be considered when identifying potential sites.

The objective of this paper is threefold: (i) to develop a knock-off criteria analysis method for the identification of candidate sites for UAM ground infrastructure, considering aeronautical feasibility requirements, accessibility and community acceptance factors, (ii) to develop and solve mathematical models for determining the optimum number, location and size of vertiports and fleet size of an on-demand reservation-based UAM system while accounting for downstream fleet operations and the interaction with passenger demand from a profit maximization and travel time savings perspective, and (iii) to the apply the proposed knock-off criteria analysis and mathematical models for the planning and operation of an UAM system in a case study in the Île-de-France/Paris region.

The remainder of this paper is organized as follows. Section 2 provides a summary of the related literature and further elaborates on the need for the proposed models. Section 3 presents the knock-off criteria, model formulations and solution approaches for the proposed formulations. Section 4 presents the results of the application of the models on the Île-de-France case study. To conclude, Section 5 presents the research conclusions, practical considerations and future research directions.

2. Literature review

The UAM system comes with various implementation and operational challenges (Rajendran and Srinivas, 2020). The decisions can be categorized into three management decision levels: strategic, tactical, and operational. Strategic decisions are long-term and are associated with high risk and expenditures, such as network design (typically several years). Tactical decisions fall in the mid-term range and involve moderate risk, such as fleet size planning (typically months to a few years). Finally, operational decisions, such as dispatching, are short-term and associated with a relatively low level of risk (typically hours to a day) (Li et al., 2020; Rajendran and Srinivas, 2020).

Fig. 1 illustrates the design levels and their interrelations. The starting point of this study is the strategic planning of UAM ground infrastructure in urban regions. While conventional aircraft acquisition is typically strategic, eVTOL fleet sizing in early-stage UAM can be adjusted more incrementally; therefore, in this study it is treated as a tactical capacity decision within the constraints of the strategic vertiport network design.

Several models and approaches are used in the literature to assess at least one of the management decisions for the planning and operation of a UAM system. The design can essentially be done through three processes: optimization, simulation and clustering algorithms. In optimization, a model is defined to search for an optimal configuration of a system, based on one or more objectives. The basis of the optimization model is a mathematical model formulation, which needs to be solved efficiently. Model size and non-linearity often prevent finding the optimal configuration in a reasonable time. An alternative are simulation approaches (including agent-based simulation), which try to

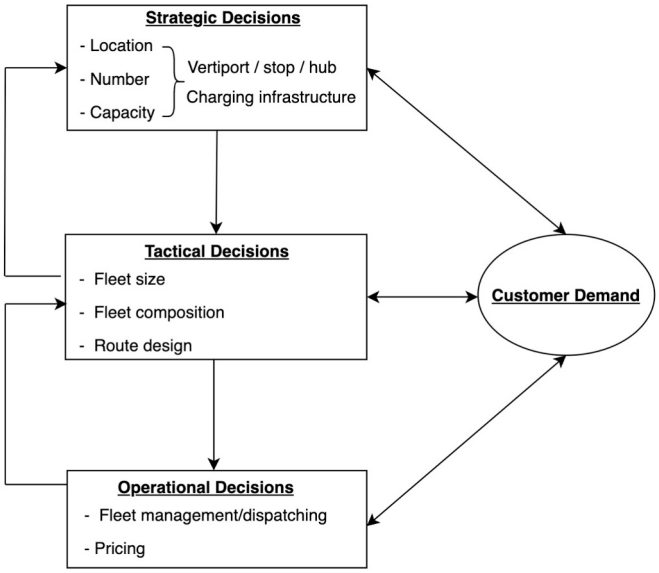

Fig. 1. UAM ecosystem management decisions.

replicate the system as best as possible. In this method, input parameters are varied to see how they influence the system performance. A drawback of the approach is that it is not suitable to find the optimal configuration, since changes in input parameters often cannot be studied together with changes in other parameters. Finally, clustering algorithms are used to cluster data to ensure higher intra-cluster similarity and lower inter-cluster similarity. A common application of this method in urban planning is the clustering of geospatial data to find optimal locations for facilities (Ikotun et al., 2023).

In the literature, models and approaches for the planning and operation of UAM systems can be classified into two broad categories: (i) models addressing strategic planning decisions and (ii) models supporting tactical and operational management decisions. The following sections explore these categories in more detail.

2.1. Models for strategic planning decisions

Strategic planning decisions relate to the location, number and capacity of vertiports, vertistops and vertihubs. A question is, for instance, whether it is best to have a more dispersed network, many small-capacity infrastructure locations to cover various demand hotspots, or a more concentrated network, a few high-capacity vertiports, for more centralized operations (Wang et al., 2022). Both networks will attract different levels of users. Therefore, it is important to consider demand-supply interaction in network design (Wu and Zhang, 2021). Another strategic decision is the location and capacity of the charging infrastructure. This decision is strongly associated with the range of the eVTOL fleet. Depending on the range, the eVTOL aircraft might be able to perform routes without recharging. This gives the possibility of expanding the network with simple vertiports without charging infrastructure at low cost (Niklab et al., 2020).

A multitude of methods have been developed to determine the optimal location and number of UAM infrastructure locations. On the optimization side, Wu and Zhang (2021) developed an extended single allocation hub-and-spoke problem to determine the optimal locations of vertiports, user allocation to vertiports and vertiports access and egress mode choice while considering the interactions between vertiport locations and UAM travel demand. The objective was to minimize the total generalized cost (travel time and cost) in the total transportation system. A similar approach was used by Rath and Chow (2022). The authors proposed a modified single allocation p-hub median location problem integrating choice-constrained user mode choice behavior for an airport shuttle service in New York. Two objectives were considered: maximizing air taxi ridership and maximizing air taxi revenue. Both studies modified typical location problems to account for demand-supply interaction. Willey and Salmon (2021) also modified the p-hub median location problem, but for another application. The authors extended the formulation by including the network dependencies on vehicle speed and battery range. A different mathematical formulation for location optimization was proposed by Boo et al. (2023). The authors developed a multi-objective and multi-period formulation with an e-constraint algorithm. The following objectives were considered: passenger accessibility, land purchase cost and service operation cost. Recently, Shon and Lee (2025) proposed a comprehensive mixed-integer programming (MIP) model that jointly addresses planning and operations in UAM systems. Their framework optimizes fleet size, vertiport parking and charging infrastructure, and eVTOL relocation across multiple time windows, accounting for spatial-temporal demand and electricity consumption.

Next to the optimization studies, clustering algorithms have been developed to assess the vertiport location problem. Rajendran and Zack (2019) proposed an iterative constrained clustering method to identify potential vertiport locations based on estimated demand for an air taxi service in New York City. In addition, the required size of vertiports to handle the clustered demand is determined. Another algorithm called CLARA was developed by Sinha and Rajendran (2023). They proposed a clustering algorithm for the phased opening of vertiport locations, while maximizing service coverage. The final clustering algorithm identified is k-means clustering. Lim and Hwang (2019) used this method to determine reasonable locations for vertiports. The input data used was commuting data.

An alternative for optimization and clustering for location optimization was proposed by Rimjha et al. (2021). The authors developed a mode-choice conditional logit model, which was used to estimate potential future UAM demand and to obtain a network of vertiports that maximizes UAM demand.

For the strategic decision related to the sizing and location of charging infrastructure in the network, a limited number of studies were found. Patel et al. (2022) developed an agent-based simulation and system dynamics model for the sizing of energy infrastructure in a UAM network, considering tactical and operations decisions on the optimal policy for deploying/charging eVTOL vehicles. An interesting characteristic of the model is that it makes a distinction between grid power and renewable energy sources. On the optimization side, Husemann et al. (2023) proposed an optimization model to analyze the cost-efficient operation of a UAM system. The model includes strategic decisions on charging infrastructure and tactical decisions on fleet composition and battery capacity. The optimization model is incorporated in a multi-agent transport simulation of the Rhine-Ruhr region, to evaluate key parameter variations via vehicle dispatching. In addition, scenario-based analyses discuss plausible UAM deployment pathways and their implications for strategic infrastructure development, including how vertiport networks and supporting energy infrastructure may evolve under different technology, policy and market conditions (Michelmann et al., 2020). A shortcoming of both studies is that the location of vertiports and corresponding charging stations is given.

2.2. Models for tactical and operational planning decisions

Tactical decisions in UAM involve determining the fleet size and composition of eVTOLs, as well as designing routes between vertiports (Li et al., 2020; Rajendran and Srinivas, 2020). Fleet sizing is a critical aspect that balances the level of service against the cost of the UAM system. This is illustrated by the trade-off of over-designing the UAM system with extra eVTOL aircraft in the fleet to serve peak periods and the extra investments in the eVTOL fleet (Garrow et al., 2021). A similar scenario is seen in the private jet sector, where fulfilling 100% of customer requests is often avoided to maintain profitability. Tactical route design decisions are influenced by the network structure, and route trajectories significantly impact air taxi travel time and the overall appeal of UAM (Niklab et al., 2020). The operational decisions relate to the routing, repositioning and charging of eVTOLs and the pricing of UAM. The price has a direct effect on the number of users. Changes in travel demand can influence the required fleet size and network size in the medium and long term (Wu and Zhang, 2021).

Multiple simulation approaches have been developed to determine the required fleet size and dispatching policy of eVTOLs and to evaluate the interaction between these design variables. Rajendran and Shulman (2020) proposed a discrete-event simulation model to determine the required number of eVTOLs balancing customer wait time and vehicle utilization. In addition, agent-based simulation has been applied to represent individual travelers and eVTOL operations in a network of vertiports and to evaluate system-wide performance under alternative infrastructure and service assumptions (Rothfeld et al., 2018). A similar study used agent-based simulation instead of discrete-event simulation to test different eVTOL dispatching logics on the fleet performance (Husemann et al., 2023). A more extensive simulation model was developed by Li et al. (2020). The authors varied, next to fleet size and fleet management policies, the vertiport capacity in a simulation model to assess UAM system performance in terms of metrics such as demand throughput and average passenger delay. The most holistic simulation model was built by Niklab et al. (2020). They developed low-fidelity

simulation models to determine the interaction between UAM components: demand, vertiport capacity, pricing and route planning. Three generic UAM networks in the metropolitan area of Munich were considered in the models.

A single optimization approach is identified in the literature that integrates both tactical and operational decisions. Shihab et al. (2020) developed a space-time network optimization approach to investigate the optimal trade-off between multiple revenue and cost sources in eVTOL fleet operations. Objectives that were considered are maximizing revenue from transporting passengers and minimizing operating and charging costs. A special characteristic of this model is that it accounts for varying electricity market prices in the dispatching of the eVTOL fleet.

2.3. Limitations of the models supporting UAM ecosystem decisions

Strong interactions exist between strategic decisions on the ground infrastructure network and corresponding charging network, tactical decisions on fleet size and composition, and operational decisions on dispatching and repositioning. For example, the required fleet size depends on the network structure and user levels. A more dispersed network necessitates more eVTOLs compared to centralized structures. Additionally, the relationship between dispatching logic and network design is significant. Determining where to position eVTOLs and how to redistribute them, considering one-way demand and parking constraints, relies on the capacities of infrastructure locations (Husemann et al., 2023). For instance, during morning peak hours, infrastructure around business districts might lack the capacity to accommodate the required number of eVTOLs simultaneously. In short, analyzing one of the decisions in isolation can lead to poor estimates of the overall system performance. The integrated framework can support municipalities and regulators, infrastructure planners and investors, and prospective UAM operators in evaluating strategic vertiport network designs while accounting for downstream fleet sizing and operational implications, and it can also inform manufacturers by indicating the minimum eVTOL capability requirements to operate in a network.

The literature review revealed that most approaches make a sharp separation between strategic management decisions on one hand and tactical/operational decisions on the other hand. This indicates that strategic decision-making models lack the integration of tactical and operational considerations, such as vehicle relocation and fleet size, which may influence the cost and performance of UAM systems. Conversely, operational models center on the detailed modelling of various dispatching strategies, presuming that factors such as location, number and size of vertiports, and fleet size are exogenously defined.

As previously introduced, Shon and Lee (2025) do propose a model that jointly addresses strategic vertiport planning and operations in UAM systems. While this represents an important step toward integrated UAM optimization, the model relies on a predefined set of vertiport locations and does not address passenger mode choice or demand-supply interaction within the optimization process. Furthermore, although the planning and operational levels are connected through steady-state decomposition, strategic factors such as vertiport site feasibility and social acceptance are assumed exogenous. Outside of the UAM literature, optimization frameworks for shared automated vehicle systems (e.g., Boyaci et al., 2015; Santos et al., 2023) and air high-speed rail intermodal networks (Lu et al., 2025) have proposed multi-level approaches that combine station location, fleet sizing, and vehicle relocation. While these approaches are methodologically relevant, they typically assume elastic demand or treat it as static. In addition, most of these models do not incorporate passenger behavioral choice through mode utility or value-of-time constructs.

Another limitation of the models is that the trade-off between the level of service offered and the total cost for implementing and operating the UAM system is not considered in the objective function. The studies either looked at the planning problem solely from a profit maximization perspective for the operator or a travel time savings perspective for the future traveler.

Lastly, Table 1 indicates how the studies identified candidate locations for vertiports. Notably, in most studies, the set of potential locations is either predefined or based on ideal placements derived from spatial demand and existing heliports. In reality, there are aeronautical feasibility requirements (Fadhil, 2018; Alves et al., 2020), community acceptance (Li, 2023; Farahani et al., 2010), land use (Vázquez, 2021; EASA, 2022) and accessibility (Fadhil, 2018) factors that need to be considered. For a realistic set of candidate vertiports, the requirements and factors need to be operationalized to spatial knock-off criteria. An interesting avenue in this respect is represented by the so-called Geographic Information Systems Multi-Criteria Decision Analysis (GIS-MCDA). This method is applied for the identification of potential sites for various applications: mobility hubs (Junyent et al., 2024; Blad et al., 2022), wind power plants (Rediske et al., 2021), health care units (Mishra et al., 2019), and bike sharing stations (Kabak et al., 2018).

As discussed in this literature review and presented in Table 1, none of the currently available models simultaneously address strategic decisions on the number, location, and capacity of vertiports, tactical decisions on fleet size, and operational decisions on the routing, repositioning, and charging of eVTOLs using optimization, while accounting for the interaction with passenger demand. This paper aims to close this literature gap, combining the perspectives of future operators and travelers.

In short, this study contributes to the current state of knowledge by introducing:

- A knock-off criteria analysis model for the identification of a realistic set of candidate locations for vertiports and corresponding maximum capacities, considering aeronautical feasibility requirements, accessibility, land use factors and impact on local communities.
- Two integer programming (IP) models that integrate strategic, tactical and operational decisions and interaction with passenger demand. Both models extend the traditional hub location problem (HLP), which is concerned with locating UAM ground infrastructure locations and allocating zones to these locations, by incorporating mode choice to account for demand-supply interaction. For this interaction, the concept of Value of Time is introduced. The formulation is further extended by incorporating time-space (TS) or time-space battery (TSB) frameworks for the modelling of downstream eVTOL operations. The frameworks differ in the level of detail with which the charging operations are modeled. In both models, the trade-off between the level of service offered and system cost is considered.

3. Model description

This section presents the formulation of the time-space and time-space-battery IP models to design an on-demand reservation-based UAM system in a regional context. eVTOLs within a specific geographic area utilize demand pooling to serve direct trips between pairs of UAM ground infrastructure locations. In what follows, a description of the system in terms of its demand and supply characteristics is given before the problem formulations are introduced. In the discussion of the supply characteristics, the knock-off criteria analysis model is presented.

3.1. System characteristics

The UAM system is characterized by several key components and constraints, as outlined below:

i. Time intervals: the entire 24-h day is divided into discrete time intervals. The first time interval starts after the last interval of the previous day. Each eVTOL operation, whether it is serving trips, charging, or relocating, starts at the beginning of a time interval and ends at the end of a time interval.

Table 1
List of referenced articles.

Reference	Supply design decisions												
	Strategic			Tactical		Operational			Method				
	Vertiport location	Vertiport capacity	Charging infrastructure	Fleet size	Route design	Fleet management	Pricing	Demand interaction	Simulation	Optimization	Choice modelling	Clustering algorithm	Method candidate vertiport selection
(Wu and Zhang, 2021)	✓							✓		✓	✓		Land-use and regulations
(Rajendran and Shulman, 2020)				✓		✓		✓	✓				Previous study
(Rajendran and Zack, 2019)	✓	✓										✓	Demand data
(Boo et al., 2023)	✓									✓			Accessibility requirements
(Rimjha et al., 2021)	✓						✓	✓			✓		None
(Shihab et al., 2020)			✓			✓		✓		✓			None
(Patel et al., 2022)			✓			✓			✓				Existing helipads and airports
(Sinha and Rajendran, 2023)	✓									✓		✓	Previous study
(Niklab et al., 2020)		✓			✓		✓		✓		✓		Land restrictions
(Husemann et al., 2023)						✓			✓				Given, no analysis
(Rath and Chow, 2022)	✓							✓		✓	✓		Given, no analysis
(Li et al., 2020)		✓		✓		✓			✓				Given, no analysis
(Willey and Salmon, 2021)	✓			✓				✓		✓			Existing helipads and airports
(Kohlman et al., 2019)				✓		✓			✓				Given, no analysis
(Lim and Hwang, 2019)	✓				✓							✓	Demand data
(Husemann et al., 2023)			✓	✓		✓	✓		✓	✓			Given, no analysis
(Michelmann et al., 2020)	✓	✓	✓					✓					Given, qualitative scenario analysis
(Rothfeld et al., 2018)		✓				✓		✓	✓				Given, no analysis
This study	✓	✓		✓		✓		✓		✓	✓		GIS knock-off criteria analysis

ii. eVTOLs: a homogeneous fleet of eVTOLs is utilized to provide services in the study area. The fleet is characterized by a maximum range, average cruising speed, passenger capacity and maximum charging speed. Note that the range positively correlates with the number of vertiport combinations that can be served. While a homogeneous fleet is assumed for simplicity and tractability, the proposed formulations can be readily extended to accommodate multiple eVTOL types with differing operational characteristics, enhancing the generalizability.

iii. UAM ground infrastructure: three archetypes of UAM ground infrastructure are considered: vertistop, vertiport and vertihub. The archetypes differ in the number of parking/charging spots, landing/take-off pads, capital and operating expenditures. A key assumption made in the models is that the capacity bottleneck lies in the number of parking/charging spots. Modelling the capacity based on the landing and take-off pad layout was too complex for this study. For the maximum capacity of the vertistop, vertiport and vertihub, earlier works by McKinsey and Company (2025) and Bluenest (2023) are consulted. They estimate the capacity at 2, 6 and 20, respectively.

The set of candidate UAM ground infrastructure locations is determined using a GIS knock-off criteria analysis in the framework presented in Fig. 2. The first step within the analysis is to handpick infrastructure types in the study area with a high potential to become UAM ground infrastructure. These infrastructure types include rooftops with parking lots, high-rise buildings, vacant land, pre-existing airports and helipads and large stadiums or concert venues (Garrow et al., 2021). Subsequently, the remaining study area is divided into a grid of cells, each measuring 100 × 100 meters. The cell approximates the size of a ground infrastructure location with the maximum capacity to handle one eVTOL (Wu and Zhang, 2021; McKinsey and Company, 2025). In other words, combining two cells results in a location with capacity for two eVTOLs. The fishnet of cells undergoes filtering using knock-off criteria, as not every cell holds the potential to become UAM ground infrastructure. Table 2 presents the knock-off criteria rules used in this paper, inspired by the latest standards and regulations and factors considered in previous studies (Fadhil, 2018; Li, 2023). Both the prohibited airspace and land use factors represent the stringent restrictions; therefore, a single knock-off rule is defined. For the existing noise, buffer to vulnerable locations and accessibility factors, multiple knock-off rules are defined, since the availability, size and effect on the filtering of the fishnet cells differ per study region. The existing noise rules are based on thresholds set by the Centers for Disease Control and Prevention (2019). In short, the knock-off criteria are hard constraints; however, because the strictness of some thresholds is uncertain, the decision-maker is advised to evaluate multiple threshold combinations.

Table 2
Knock-off criteria.

Factor	Rule	Description
Prohibited airspace	PA	Vertiport must not be located in prohibited airspace for helicopters
Land use	LU	Vertiport must not be located in land use areas of individual housing, collective housing, retail districts, industrial areas, existing transport infrastructure and quarries, landfills and construction sites.
Existing noise[1]	N1	Existing noise in urban areas ≥ **60 dB**
	N2	Existing noise in urban areas ≥ **70 dB**
	N3	Existing noise in urban areas ≥**80 dB**
Buffer vulnerable locations	BS1	≥ **500 m** buffer from schools
	BS2	≥ **750 m** buffer from schools
	BS3	≥ **1000 m** buffer from schools
	BH1	≥ **500 m** buffer from hospitals
	BH2	≥ **750 m** buffer from hospitals
	BH3	≥ **1000 m** buffer from hospitals
Accessibility[2]	A1	≥ **500 activity locations** in 5-km radius
	A2	≥ **1000 activity locations** in 5-km radius
	A3	≥ **1500 activity locations** in 5-km radius

[1] A vertiport must be situated in an area where the existing noise levels exceed a specified threshold to mitigate the overall noise impact.
[2] Activity locations include areas designated for home, work, education, shopping, and other purposes.

Following the GIS knock-off criteria analysis, the remaining cells serve as input for a candidate vertiport selection algorithm with 9 steps, illustrated in Fig. 3. The goal of this algorithm is to identify a set of candidate UAM ground infrastructure locations by aggregating individual fishnet cells, subject to a user-specified minimum separation distance between locations and a maximum allowable number of locations. The first step is to compute for each remaining cell an attractiveness score. This score is a function of the accessibility score (number of activity locations in a 5-km radius) and the capacity potential. The capacity potential of a cell is determined by the number of cells adjacent to the selected cell and the cells adjacent to those and so forth. Once the attractiveness score for each cell is determined, the subsequent step involves selecting the cell with the highest attractiveness score (1). Next, adjacent cells are added to the cells belonging to the UAM ground infrastructure location, until no more adjacent cells are found, or the maximum capacity of the biggest vertihub archetype is reached (2). In step 3, all candidate cells within a user-specified radius of the set of cells belonging to the selected infrastructure locations, representing the minimum distance between vertiports, are removed. Finally, in step 4, a

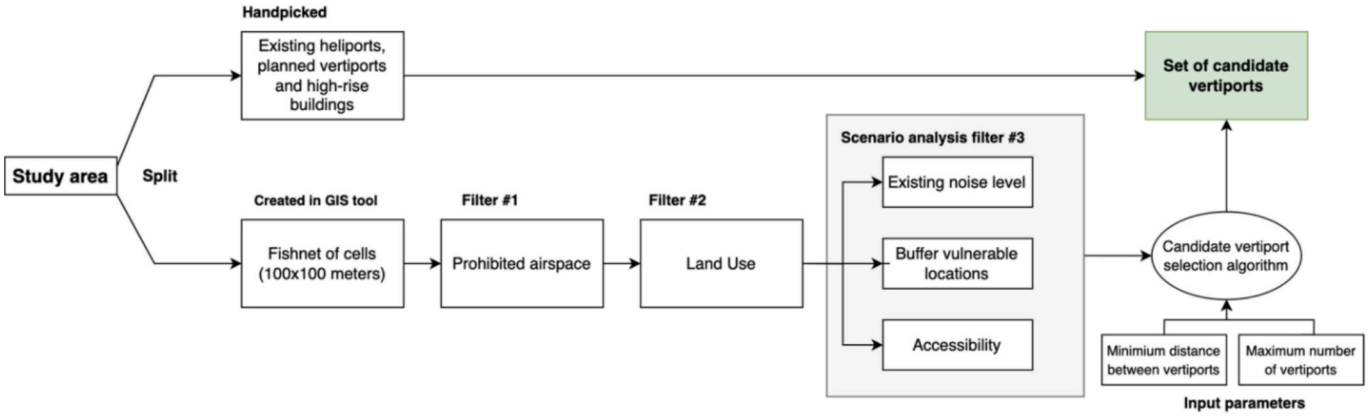

Fig. 2. Steps to determine set of candidate UAM ground infrastructure locations.

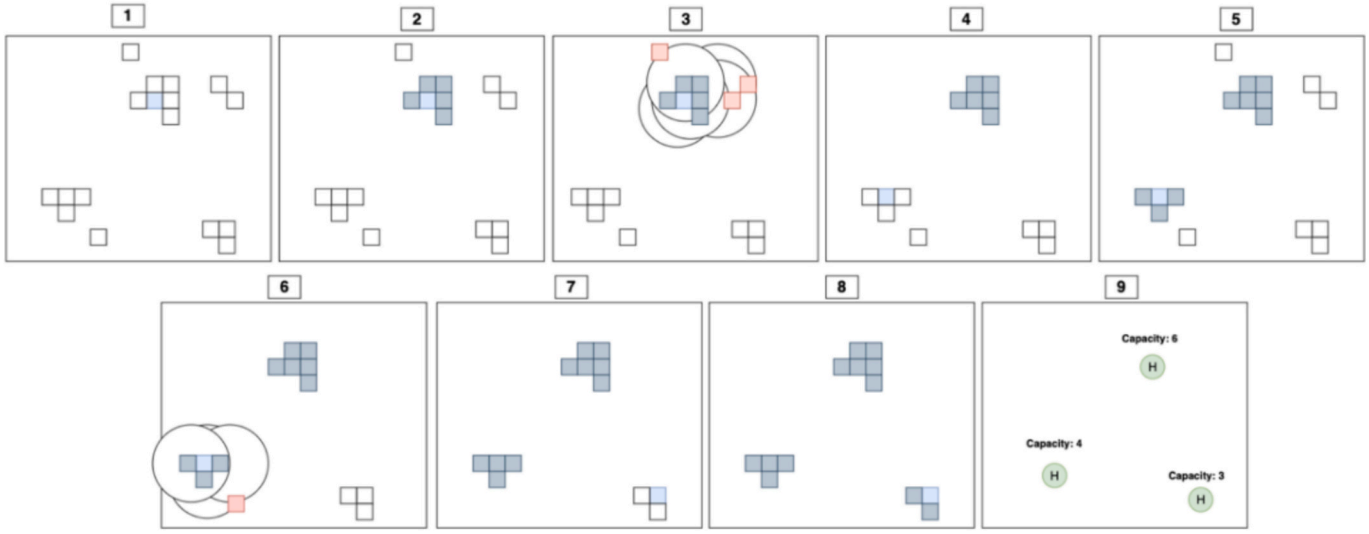

Fig. 3. Candidate vertiport selection algorithm.

new cell with the highest attractiveness score from the remaining set of candidate cells is selected, initiating a new iteration, repeating steps 5 and 6. The algorithm converges when no fishnet cells remain or the maximum number of infrastructure locations is reached. The final output is a set of candidate UAM ground infrastructure locations, categorized by their capacity potential: vertistop, vertiport, and vertihub.

iv. eVTOL routes: the travel time between ground infrastructure locations depends on the routing between the locations and the eVTOL speed. This routing is dependent on the design and use of the airspace and interaction with other flying vehicles (Li et al., 2020). Based on recent UAM developments, the expectation is that eVTOLs will first operate under current ATM procedures and Visual Flight Rules (VFR) (Schweiger and Preis, 2022). Therefore, the travel time is determined by creating a network of routes between the infrastructure locations. This network considers existing helicopter corridors, restricted airspaces and the presence of highways or railway lines. The network aims to find realistic travel times that mitigate the noise impact on local communities.

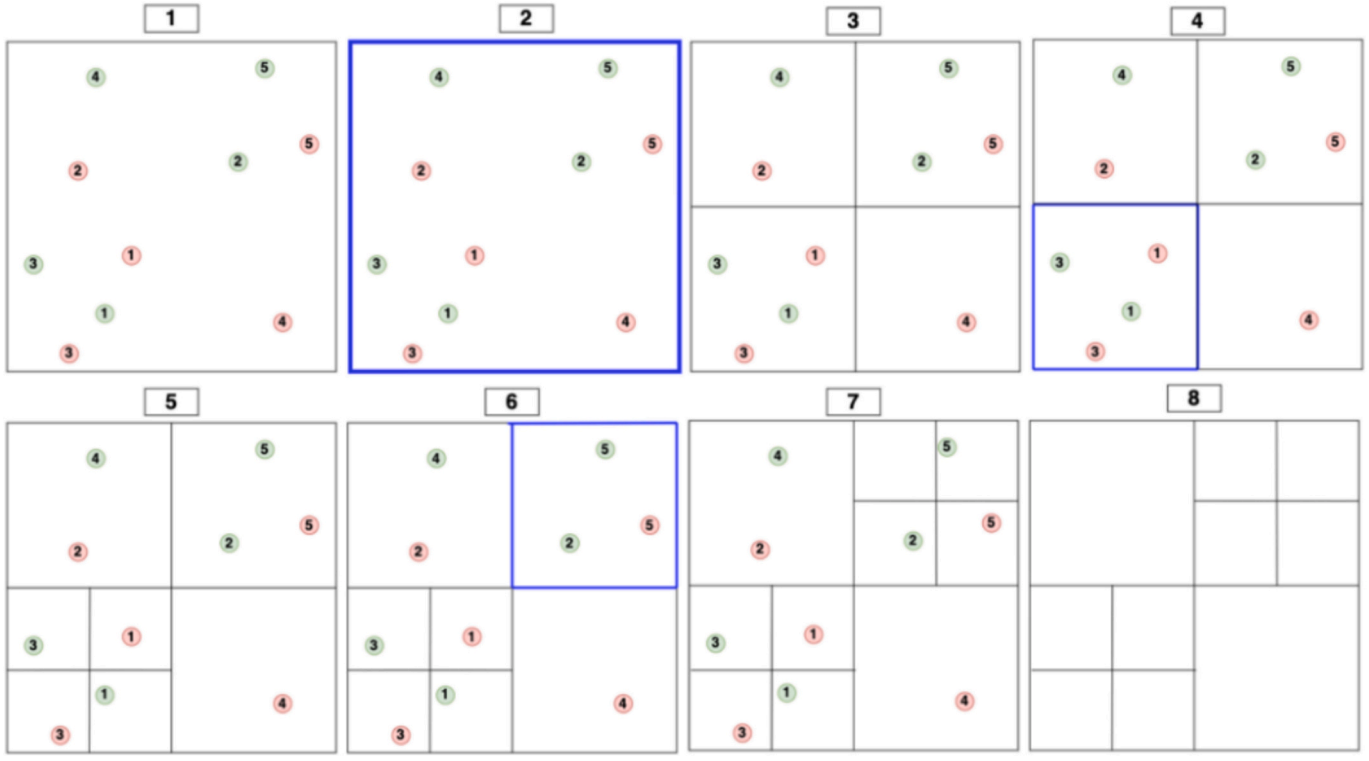

Fig. 4. Depiction zoning algorithm.

v. Demand: the travel demand for a study region can be obtained using the synthetic population and travel demand pipeline developed by Hörl and Balac (2021). The pipeline is notable for its reproducibility and applicability to various regions worldwide, as it relies solely on publicly accessible data and software. The data sources include population, enterprise, service, and facility census, addresses, household travel surveys and tax registries. The output of the pipeline is a set of trips over the day, including origin and destination coordinates, travel mode and trip purpose, and information about the socio-economic characteristics of the traveler carrying out the trip.

To decide whether a trip has the potential to be carried out by a UAM service, the concept of Value of Time (VoT) is introduced. The VoT represents, in this context, the monetary value associated with the travel time saved by travelers using a faster mode. A trip qualifies for UAM if it results in a net reduction in the generalized travel cost, which combines the travel cost and the travel time converted to cost using the VoT. Note that the travel time and cost of UAM include both the access/egress and UAM segments. Given the modelling complexity, the walk and taxi modes are only considered as access/egress modes. To account for heterogeneity in the valuation of time, the population is divided into multiple population segments using the trip and socio-economic characteristics of the synthetic pipeline. For instance, high-income car users doing a long-distance business trip have a higher VoT compared to low-income public transport users doing a short leisure trip. Within each population segment, we apply a single VoT to all trip components (access/egress and UAM). Allowing VoT to differ by trip component could be considered in future work.

vi. Zones: the daily trips from individual households from the synthetic population and travel demand pipeline are presented as origin and destination coordinates. Given computational resource restrictions, the individual trips need to be aggregated into zones. For the zoning, a gradual rasterization algorithm is applied, illustrated in Fig. 4. The objective of this algorithm, inspired by Moeckel and Donnely (2015), is to determine the minimum number of zones needed without sacrificing information. Information loss could occur if potential UAM trips occur within the same zone. Potential daily trips can be identified using the Value of Time concept introduced in v. Demand, based on the most attractive UAM pricing scenario. The initial step in the algorithm involves data generation, in which the origin and destination coordinates are placed within a designated study area (1). The green and red dots represent the origin and destination points of each trip, respectively. In the beginning, a single raster cell, representing a zone, is overlaid onto the study area (2). During the rasterization, the inter-flow percentage is computed for the study area. If the percentage is not equal to the set threshold, the cell with the highest number of intra-zonal trips is chosen. This cell is then divided into four new raster cells (3). This process iterates until the set threshold in the entire study area is met (4–6). Steps 7 and 8 show the final zoning structure.

The result of the zoning algorithm is an origin-destination matrix for each population segment and time interval. In the case a particular population segment opts to choose the UAM service for an OD pair, a reservation is made for the next day.

vii. Dispatching/system controller: the dispatcher, based on the incoming requests in the reserving period of the previous day, assigns tasks to the eVTOL fleet, including serving trips, relocating, and charging for the whole day. The dispatcher has the discretion to either fulfil or reject requests. Pooling is handled only for requests with the same origin–destination (OD) pair, since the dispatcher is restricted to direct flights and is not allowed to route passengers through intermediate UAM ground infrastructure locations. No passenger waiting or queueing process is modeled explicitly. Instead, pooling is represented through the time discretization: depending on the chosen time-interval length, the dispatcher can bundle requests within a limited time window around a planned departure and assign them to the same flight. The resulting dispatch plan determines the set of served trips, relocations, and charging actions over the day.

viii. Operations:

a. **Serving trips:** when an individual trip request between a pair of ground infrastructure locations at the beginning of a time interval is accepted, the eVTOL is deployed to fulfil the trip. It is assumed that each trip commences at the beginning of a time interval and concludes within the same or in the subsequent intervals, depending on the size of the time interval. The eVTOL can fulfil multiple trip requests at the same time, depending on its capacity and the size of the demand. The travel time between UAM ground infrastructure locations includes the flying time and the boarding/deboarding time of passengers.
b. **Relocation:** relocation can be implemented to rebalance the eVTOLs within the system. This may be required when accumulation and/or shortages of eVTOLs occur at UAM ground infrastructure locations, potentially due to the one-way nature of demand throughout the day.
c. **Charging:** the electric batteries of eVTOLs need to be charged. At the start of the service period, each eVTOL is initialized as fully charged in the model. In Model 1, which uses a time-space formulation, the eVTOL fully charges after each relocation or trip-serving operation. The duration of charging, measured in time intervals, depends on the distance covered during the previous flight. Model 2 divides the battery capacity into equal levels to create a time-space-battery formulation. The eVTOL can perform multiple flight legs if the battery level is sufficient. Both models consider the battery consumption to be linear during trip serving and relocations. Charging time is thus accounted for through (i) required charging intervals in Model 1 and (ii) battery-level transitions with a charging rate per time interval in Model 2. If an eVTOL enters a ground infrastructure point and is connected to a charger, it occupies the parking/charging spot until it leaves the point. Even if the battery is fully charged, the eVTOL remains connected to the parking/charging spot until the eVTOL is assigned for relocation or for serving trips.

ix. Costs and revenues: the model consists of two objectives, reflecting the perspectives of the operator and the traveler, creating a multi-objective problem. The perspective of the operator is expressed in the daily profit, which combines the service revenue with the fixed and variable vehicle costs and the cost of operating a ground infrastructure location. The perspective of the traveler is expressed in the generalized travel cost savings.

a **Service Revenue:** travelers must pay a service price to use the UAM service between a pair of ground infrastructure locations. The service price consists of a base fare and a passenger-kilometer fare.
b **Fixed eVTOL cost:** the fixed cost associated with operating an eVTOL is composed of depreciation, cleaning and insurance costs.
c **Variable eVTOL cost:** the variable cost comes with operating an eVTOL per kilometer between vertiports. This includes energy, maintenance and personal cost.
d **UAM ground infrastructure operating cost:** the operating cost depends on the archetype. McKinsey & Company (n.d.) has made estimations on the capital and operating expenditures per archetype. The capital expenditures represent the cost of building the ground infrastructure archetype and associated equipment such as charging spots, terminal buildings and landing and take-off pads. The operating expenditures include the maintenance, security and personnel costs.
e **Generalized travel cost savings:** the generalized travel cost is the sum of the travel cost and travel time. To sum both components, the travel time is translated into a monetary cost using the VoT. The total generalized travel cost savings are determined by comparing the new

generalized travel cost of UAM users with their existing ground transportation alternative for a specific origin-destination pair. In other words, the generalized travel cost savings represent the level of service provided by the UAM system to each particular population segment.

3.2. Mathematical formulation – Model 1: time-space flow-based IP model

Here we present the mathematical structure of the first proposed model, that is, the time-space flow-based IP model. Vertiport planning is quite similar to the design of on-demand one-way car-sharing systems and bike-sharing systems. Lessons can be learned from the literature in this field on how to simultaneously model decisions related to determining station location, size, number, and fleet size, while considering the dynamics of vehicle relocation, charging operations, and system balancing for a reservation-based system. The model is inspired by car-sharing frameworks developed by Boyaci et al. (2015) and Correia and Antunes (2012). In this section, first the sets and indices, as well as the function, variables, and parameters are presented. This is followed, in Section 3.2.2, by a detailed description of the multi-objective mathematical model with its objectives, functions and constraints.

3.2.1. Inputs

Sets and indices	
$k, m \in V_h$	Set of potential vertiport nodes
$i, j \in V_d$	Set of potential demand nodes
$p \in P$	Set of population segments
$t, u, w \in T$	Set of time intervals
$u \in U$	Set of UAM ground infrastructure archetypes
Parameters	
VoT_p	Value of time of population segment p [€/hour]
Pr_{km}	Service price to transport one user between UAM ground infrastructure locations k and m [€]
CM_{km}	Cost of moving one eVTOL between UAM ground infrastructure locations k and m, which includes energy and personal cost [€]
CV	Daily fixed cost per eVTOL (depreciation, insurance and cleaning) [€]
CP_u	Daily operating cost of an UAM ground infrastructure type u.Combination of capital (installation and equipment) and operating (maintenance, personal, security) expenditures. [€]
TT_{ikp}	Travel time between demand node i and UAM ground infrastructure point k for population segment p of best access/egress mode [hours]
TC_{ikp}	Travel cost between demand node i and UAM ground infrastructure point k for population segment p of best access/egress mode [€]
TT_{km}	Travel time using an eVTOL between UAM ground infrastructure locations k and m [hours]. The travel time includes the flying time between the ground infrastructure locations, denoted as TF_{km} and time spend by passengers waiting, transferring and boarding and deboarding the eVTOL, denoted as TW. The total travel time is calculated as followed $TT_{km} = TF_{km} + TW$
TC_{km}	Cost for traveler for using an eVTOL between UAM ground infrastructure locations k and m [€]
TT_{ijp}	Travel time using best pure ground transportation mode of population segment p between demand nodes i and j [hours]
TC_{ijp}	Travel cost using best pure ground transportation mode of population segment p between demand nodes i and j [€]
OD_{ijpt}	Travel demand between origin and destination nodes i and j of population segment p at the beginning of time interval t [#]
$ECAP$	The capacity of an eVTOL in terms of the number of passengers. All eVTOLs have the same capacity [#]
$VCAP_k$	Maximum capacity of vertiport k, retrieved from the GIS-analysis [#]
$ACAP_u$	Capacity of UAM ground infrastructure archetype u [#]
CP^{tu}_{km}	Binary vector for charging periods after eVTOL trip between UAM ground infrastructure locations k and m from the beginning of time interval t to the end of time interval u
$CLOSE^{tu}_{km}$	Binary parameter indicating whether trip between UAM ground infrastructure locations k and m from the beginning of time interval t to the end of time interval u falls within ($CLOSE^{tu}_{km} = 0$) or outside ($CLOSE^{tu}_{km} = 1$) the night closure
w_P	Weight perspective of the operator expressed in daily profit
w_{GC}	Weight perspective of the traveler expressed in generalized travel cost savings

(*continued on next column*)

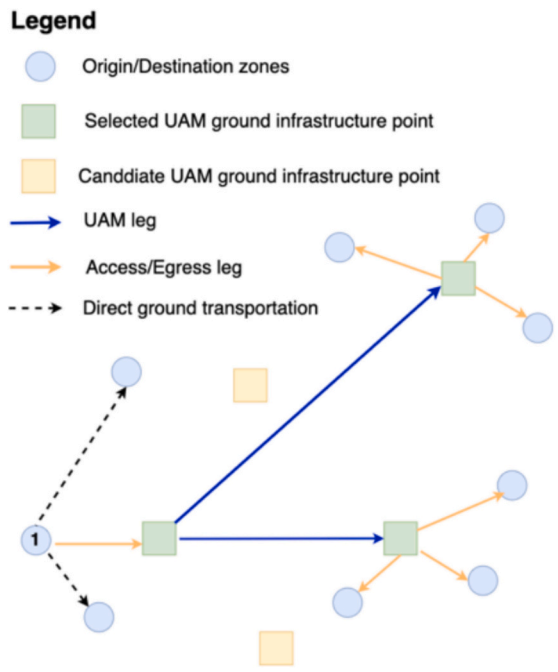

Fig. 5. Hub-and-Spoke network structure.

(*continued*)

M	Big number
Function	
$betwn(t, u)$	Set of time intervals between the beginning of time interval t and the end of time interval u.
Decision variables	
a_{ijkp}	Binary variable indicating if population segment p between demand nodes i and j uses ground infrastructure point k ($a_{ijkp} = 1$) or not ($a_{ijkp} = 0$) (Access)
b_{ijkp}	Binary variable indicating if population segment p between demand nodes i and j uses ground infrastructure point k ($b_{ijkp} = 1$) or not ($b_{ijkp} = 0$) (Egress)
$h_{k,u}$	Binary variable indicating if ground infrastructure point k opened with UAM ground infrastructure archetype u ($h_{k,u} = 1$) or not ($h_{k,u} = 0$)
y^t_{ijkmp}	Number of trips accepted between demand nodes i and j through ground infrastructure location k and m for population segment p at the beginning of time interval t
z^{tu}_{km}	Number of eVTOLs used for serving trips between ground infrastructure location k and m at the beginning of time interval t and the end of time interval u
r^{tu}_{km}	Number of eVTOLs relocated between ground infrastructure location k and m at the beginning of time interval t and the end of time interval u.
Auxiliary variables	
n^t_k	Number of eVTOLs available in ground infrastructure point k at the beginning of time interval t
e_{ijp}	Binary variable indicating if population segment p between demand nodes i and j uses pure ground transportation ($e_{ijp} = 1$) or not ($e_{ijp} = 0$)
x_{ijkmp}	Binary variable indicating if population segment p between demand nodes i and j uses UAM between vertiport k and m ($x_{ijkmp} = 1$) or not ($x_{ijkmp} = 0$)
v	Number of eVTOLs in system
s^t_{ijkmp}	Number of trips rejected between demand nodes i and j through vertiports k and m for population segment p at the beginning of time interval t
l_t	Number of eVTOLs serving demand before time interval t which are still serving demand during time interval t
g_t	Number of eVTOLs being relocated during time interval t for which their relocation started before t

3.2.2. Detailed model

$$f_1 = \overbrace{\sum_{i,j\in V_d}\sum_{k,m\in V_h}\sum_{t\in T}\sum_{p\in P}\left(Pr_{km}\cdot y^t_{ijkmp}\right)}^{\text{Service revenue}} - \overbrace{\sum_{k,m\in V_h}\sum_{t\in T}\left(CM_{km}\cdot\left(z^{tu}_{km}+r^t_{km}\right)\right)}^{\text{Operation/relocating cost eVTOL}} - \overbrace{CV\cdot v}^{\text{Daily fixed eVTOL cost}} - \overbrace{\sum_{u\in U}\sum_{k\in V_h}\left(\mathrm{CP}_u\cdot h_{k,u}\right)}^{\text{Daily operating cost vertiport}} \tag{I.1}$$

$$f_2 = \overbrace{\sum_{i,j\in V_d}\sum_{p\in P}\sum_{t\in T}\left(\left(TT_{ijp}\cdot VOT_p + TC_{ijp}\right)\cdot OD_{ijpt}\right)}^{\text{Total generalized travel cost without UAM service}} - \overbrace{\sum_{i,j\in V_d}\sum_{k,m\in V_h}\sum_{t\in T}\sum_{p\in P}\left(\left(\left(\left(TT_{km}+TT_{ikp}+TT_{jmp}\right)\cdot VOT_p\right)+TC_{km}+TC_{ikp}+TC_{jmp}\right)\cdot y^t_{ijkmp}\right)}^{\text{Generalized travel cost with UAM service:satisfied demand}} - \tag{I.2}$$

$$\overbrace{\sum_{i,j\in V_d}\sum_{k,m\in V_h}\sum_{t\in T}\sum_{p\in P}\left(\left(TT_{ijp}\cdot VOT_p + TC_{ijp}\right)\cdot s^t_{ijkmp}\right)}^{\text{Generalized travel cost with UAM service:unsatisfied demand}} - \overbrace{\sum_{i,j\in V_d}\sum_{p\in P}\sum_{t\in T}\left(\left(TT_{ijp}\cdot VOT_p + TC_{ijp}\right)\cdot e_{ijp}\cdot OD_{ijpt}\right)}^{\text{Generalized travel cost with UAM service:ineligible demand}}$$

$$\max w_P\cdot f_1 + w_{GC}\cdot f_2 \text{ where } w_P + w_{GC} = 1 \tag{I.3}$$

Subject to:

$$e_{ijp} + \sum_{k\in V_h} a_{ijkp} = 1\ (\boldsymbol{a})\quad e_{ijp} + \sum_{k\in V_h} b_{ijkp} = 1\ (\boldsymbol{b}) \qquad \forall\, i,j\in V_d, p\in P \tag{I.4}$$

$$a_{ijkp} - \sum_{m\in V_h, m\neq k} x_{ijkmp} = 0\ (\boldsymbol{a})\quad b_{ijkp} - \sum_{m\in V_h, m\neq k} x_{ijmkp} = 0\ (\boldsymbol{b}) \qquad \forall\, i,j\in V_d, p\in P, k\in V_h \tag{I.5}$$

$$\mathrm{a}_{\mathrm{ijkp}} \leq \sum_{u\in U} h_{k,u}\ (\boldsymbol{a})\quad b_{ijkp} \leq \sum_{u\in U} h_{k,u}\ (\boldsymbol{b}) \qquad \forall i,j\in V_d, p\in P, k\in V_h \tag{I.6}$$

$$TT_{ijp} - \sum_{k\in V_h}\left(TT_{ikp}\cdot a_{ijkp} + TT_{jkp}\cdot b_{ijkp} + \sum_{m\in V_h}\left(TT_{km}\cdot x_{ijkmp}\right)\right)\cdot VOT_p \geq \sum_{k\in V_h}\left(TC_{ikp}\cdot a_{ijkp} + TC_{jkp}\cdot b_{ijkp} + \sum_{m\in V_h}\left(TC_{km}\cdot x_{ijkmp}\right)\right) - TC_{ijp}$$
$$-$$
$$- \qquad \forall i,j\in V_d, p\in P \tag{I.7}$$
$$-$$

$$y^t_{ijkmp} + s^t_{ijkmp} = x_{ijmkp}\cdot OD_{ijpt} \qquad \forall i,j\in V_d, k,m\in V_h, t\in T \tag{I.8}$$

$$n^t_k \leq \sum_{u\in U} ACAP_u\cdot h_{k,u} \qquad \forall k\in V_h, t\in T \tag{I.9}$$

$$ACAP_u\cdot h_{k,u} \leq VCAP_k \qquad \forall k\in V_h, u\in U \tag{I.10}$$

$$\sum_{u\in U} h_{k,u} \leq 1 \qquad \forall k\in V_h \tag{I.11}$$

$$\sum_{i,j\in V_d}\sum_{p\in P} y^t_{ijkmp} \leq z^{t(t+TT_{km})}_{km}\cdot ECAP \qquad \forall k,m\in V_h, t\in T \tag{I.12}$$

$$n^t_k \geq \sum_{m\in V_h}\sum_{u\in T} z^{tu}_{km} + \sum_{m\in V_h}\sum_{u\in T} r^{tu}_{km} \qquad \forall k\in V_h, t\in T \tag{I.13}$$

$$n^t_k - \sum_{m\in V_h}\sum_{u\in T} z^{tu}_{km} + \sum_{m\in V_h}\sum_{u\in T} z^{ut}_{mk} - \sum_{m\in V_h}\sum_{u\in T} r^{tu}_{km} + \sum_{m\in V_h}\sum_{u\in T} r^{ut}_{mk} = n^{t+1}_k \qquad \forall k\in V_h, t\in T \tag{I.14}$$

$$n^t_k \geq \sum_{(k,m,u,w):t\in CP^{inw}_{mk}} z^{inw}_{mk} \qquad \forall k\in V_h, t\in T \tag{I.15}$$

$$\sum_{(k,m,u,w):t\in betwn(tu)\setminus u} z^{inw}_{km} = l_t\ (\boldsymbol{a})\ \sum_{(k,m,u,w):t\in betwn(tu)\setminus u} r^{inw}_{km} = g_t\ (\boldsymbol{b}) \qquad \forall t\in T \tag{I.16}$$

$$\sum_{k\in V_h} n^t_k + l_t + g_t = v \qquad \forall t\in T \tag{I.17}$$

$$z^{tu}_{km} + r^{tu}_{km} \leq M\cdot CLOSE^{tu}_{km} \qquad \forall k,m\in V_h, t,u\in T \tag{I.18}$$

$$a_{ijkp}, b_{ijkp}, e_{ijp}, x_{ijkmp}, h_{k,u} \in \{0,1\} \qquad \forall i,j\in V_d, p\in P, k,m\in V_h, u\in U \tag{I.19}$$

$$y^t_{ijkmp}, s^t_{ijkmp}, r^{tu}_{km}, z^{tu}_{km}, l_t, g_t \in N \qquad \forall i,j\in V_d, p\in P, k,m\in V_h, t,u\in T \tag{I.20}$$

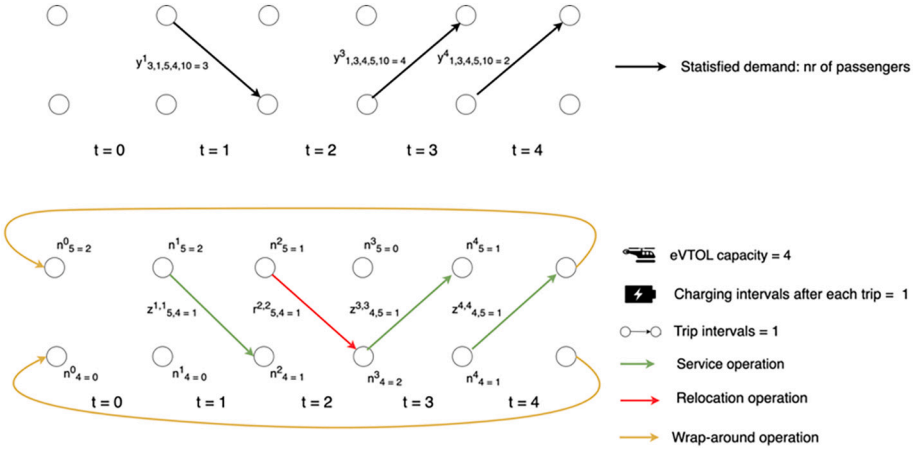

Fig. 6. Illustration time-space network.

The model is described in Eq. (I.1)-(I.20). The first objective (Eq. (I.1)) expresses the objective function of the daily profit of the operator. Revenue is computed solely from the satisfied demand between UAM ground infrastructure locations and the service price for travelling between these locations. The first cost component involves the variable vehicle cost of serving trips and relocating eVTOLs. The second and third cost components are, respectively, the fixed vehicle cost and the ground infrastructure operating cost. The total number of eVTOLs in the system is used for the fixed eVTOL cost. The ground infrastructure operating cost is determined by the number of opened locations per archetype multiplied by the corresponding daily operating cost per archetype.

The second objective (Eq. (I.2)) calculates the generalized travel cost savings by introducing the UAM system. Initially, the total generalized travel cost in the system is determined with no UAM system. Subsequently, the total generalized travel cost when the UAM system is introduced is computed, comprising three parts: the generalized cost of the satisfied demand that is transported with eVTOLs, the generalized travel cost for rejected travel demand that still need to use the current ground transportation mode and finally the generalized travel cost of ground transportation of the population segments and origin-destination pairs that did not opt to use UAM. Both objectives are expressed in monetary terms, facilitating the possibility of creating a multi-objective function, as illustrated in Eq. (I.3). The weights w_P and w_{GC} represent the importance of the operator's and traveler's objectives, respectively. Both weights should sum up to 1.

Constraints (I.4)–(I.7) relate to the hub-and-spoke network problem, in which the routes for each population segment are determined. Fig. 5 gives an overview of the hub-and-spoke structure by showing the routing from zone 1 to the other zones. Constraints (I.4a)–(I.4b) correspond to the two routing options illustrated in the figure: for each OD pair and population segment, demand is either assigned to the ground alternative with a direct ground connection between origin and destination, or assigned to the UAM alternative, in which the trip is routed via an origin-side and a destination-side UAM ground infrastructure point through an access leg, a flight leg, and an egress leg. Constraints (I.5a) and (I.5b) are routing conservation constraints. In Fig. 5, these constraints ensure that whenever the UAM alternative is chosen for an OD pair, the selected access, flight, and egress legs form one consistent path and that no incomplete routing is allowed. Constraints (I.6a) and (I.6b) ensure that UAM routing can only use UAM ground infrastructure locations that are opened by the model, which is illustrated in the figure by the distinction between selected (green) and non-selected (yellow) candidate locations. Constraints (I.7) represent an important backbone of the model. This constraint ensures that a population segment can only opt for UAM between origin and destination i and j, if the value of travel time savings compared to their current transportation alternative is higher than the additional cost that is associated with UAM.

Constraints (I.8)–(I.18) are the constraints associated with the flow-based time-space network. Fig. 6 provides an illustration of the mechanisms of the network and the role of the different decision variables. In the figure, the top panel illustrates demand satisfaction over time, while the bottom panel illustrates the corresponding eVTOL flow decisions. Constraints (I.8) form the bridge between the hub-and-spoke problem and the time-space network. It ensures that the demand for travelers who opt to choose UAM either needs to be satisfied or remain unsatisfied for different time intervals during the day. For illustration, only the satisfied demand is depicted in the top panel of Fig. 6, shown as black arcs.

Constraints (I.9) ensure that the number of available eVTOLs at a UAM infrastructure point k of archetype u is not higher than the capacity of that archetype. Constraints (I.10) ensure that the archetype selected at a UAM ground infrastructure k is not higher than the maximum capacity, obtained from the GIS-analysis, which translates the physical capacity of that location. Constraints (I.11) ensure that a maximum of one archetype is chosen per candidate UAM ground infrastructure point k.

Constraints (I.12) ensure that in case demand is satisfied between a pair of vertistops from the beginning of a certain interval to the end of a certain interval, an eVTOL needs to be operated to serve this demand. This is illustrated in Fig. 6 by the trip-serving arcs in the bottom panel (green), which correspond to satisfied-demand arcs in the top panel. Constraints (I.13) ensure that the number of eVTOLs that leave UAM ground infrastructure point k at the beginning of time interval t for serving trips or relocation cannot be higher than the number of available eVTOLs at the specific ground infrastructure location. Constraints (I.14) impose standard eVTOL flow conservation at each UAM ground infrastructure location. In each time interval, the number of eVTOLs present equals those arriving plus those carried over from the previous interval, and these eVTOLs must either remain at the location or depart to another location in the next interval. Constraints (I.15) are more complex and account for the charging of eVTOLs. For each eVTOL trip, the number of charging periods is determined and is proportional to the trip distance. These constraints ensure that the number of available eVTOLs at each vertiport k and time interval t is greater than the number of eVTOLs being charged at that location and time. Consequently, eVTOLs arriving at a vertiport cannot immediately depart again. Fig. 6 illustrates this principle. After completing a trip and any necessary relocation operation, an eVTOL must charge for one interval. Therefore, the relocation must begin at the start of time interval 2 to ensure the eVTOL is ready to serve trips at the beginning of time interval 4.

Constraints (I.16a) and (I.16b) keep track of the number of eVTOLs that are respectively serving trips or relocating at the beginning of time interval t, but started this operation before time interval t. Combining the number of eVTOLs in operation at the beginning of time interval t

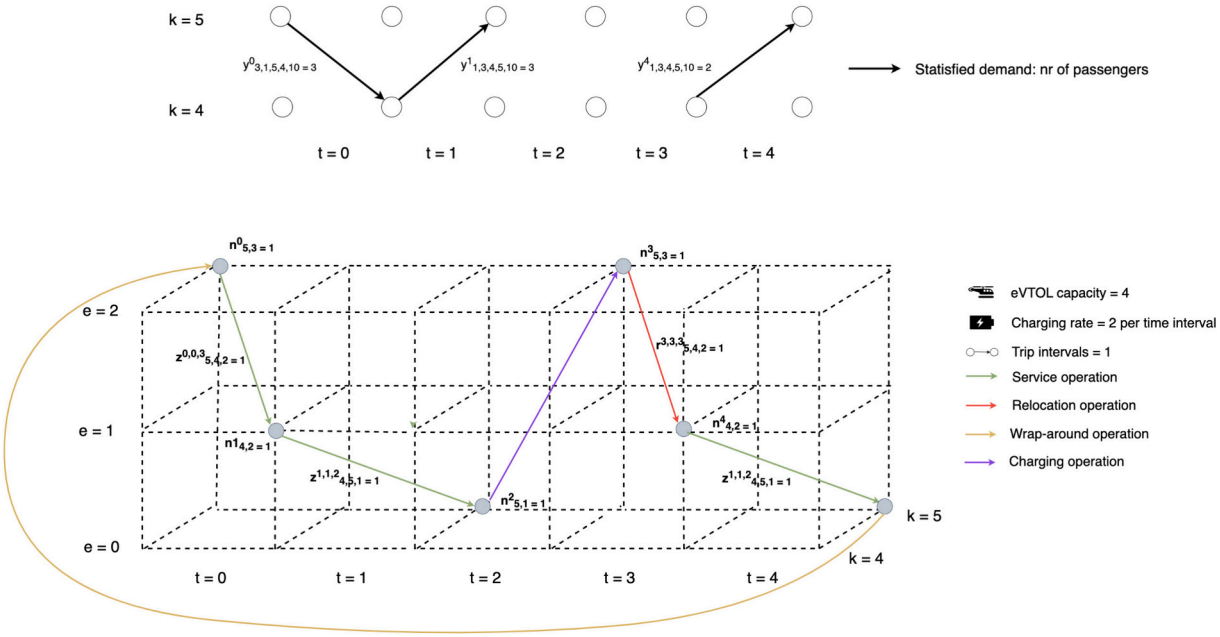

Fig. 7. Illustration time-space-battery network.

Table 3
Number of decision variables per set.

Decision variable sets	Number of variables
a_{ijkp}	$(V_d^2 - V_d) \bullet V_h$
b_{ijkp}	$(V_d^2 - V_d) \bullet V_h$
h_k	V_h
c_k	V_h
y^t_{ijkmp}	$(V_d^2 - V_d) \bullet (V_h^2 - V_h) \bullet P \bullet T$
z^{tu}_{km}	$(V_h^2 - V_h) \bullet (T^2 - T)/2 + V_h$
r^{tu}_{km}	$(V_h^2 - V_h) \bullet (T^2 - T)/2 + V_h$
z^{tue}_{kmf}	$(E^2 - E)/2 \bullet (V_h^2 - V_h) \bullet (T^2 - T)/2 + V_h$
r^{tue}_{kmf}	$(E^2 - E)/2 \bullet (V_h^2 - V_h) \bullet (T^2 - T)/2 + V_h$

with the number of available eVTOLs at each vertiport at the beginning of time interval t gives the total number of eVTOLs, see constraints (I.17). Constraints (I.18) ensure that there are no trip serving or relocation operations during the night closure. Finally, expressions (I.19), (I.20) set the domain for the decision variables.

3.3. Mathematical formulation – Model 2: time-space-battery flow-based IP model

Model 2, the time-space-battery flow-based IP model, expands Model 1 with a more detailed modelling of the charging operation of the eVTOLs. In the expanded model, a new set E is introduced, which divides the battery capacity into $E + 1$ equal levels, where $E = \{0, 1, 2, \ldots, E\}$. A 100% battery charging level corresponds to level E. In addition, two new parameters are added, c_{km} and *rate*. The parameters represent, respectively, the number of energy levels E consumed between UAM ground infrastructure location k and m, and the number of energy levels E charged per time interval. The flow decision variables z and r are indexed with two additional indices e and f from the new energy levels set, representing the starting and ending battery level of a trip serving and relocation operation. Next to the flow decision variables, the auxiliary variable n is indexed with battery level e. The variable now keeps track of the number of available eVTOLs at a vertiport at the beginning of a time interval with a specific battery level, creating a space-time-battery network.

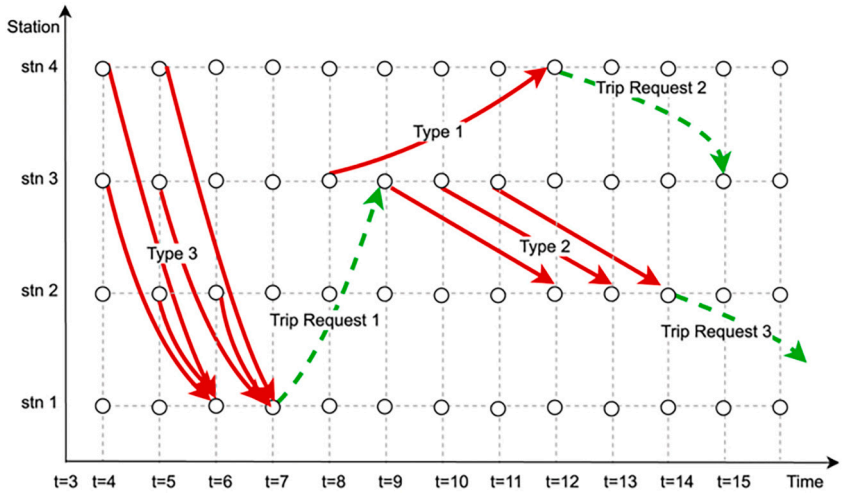

Fig. 8. Model size reduction: relocation restriction (Bekli et al., 2021).

A large portion of the constraints of Model 1 are adopted in Model 2. However, multiple constraints had to be altered to account for the space-time-battery structure. In Table ..., the new constraints of Model 2 and the number of original constraints in Model 1 are presented. The dynamics of the time-space-battery framework are inspired by previous work in car-sharing systems by Bekli et al. (2021) and Santos et al. (2023).

constraints (II.4), (II.5), (II.6). All constraints ensure that the number of eVTOLs at infrastructure point k at the beginning of time interval t with battery level e is equal to the number of eVTOLs available at time $t+1$ with battery level $e + rate$ minus the eVTOLs leaving for serving trips and relocating at the beginning of time interval t and plus the eVTOLs arriving at the end of time interval t with battery level $e + rate$. Note that these constraints are written separately for cases where $e + rate < E$, E and $e < E$.

		Model 1 constraint number	Model 2 constraint number
$\sum_{e\in E} n^t_{ke} \le \sum_{u\in U} ACAP_u \cdot h_{k,u}$	$\forall k \in V_h, t \in T$	(I.9)	(II.1)
$\sum_{i,j\in V_d}\sum_{p\in P} y^t_{ijkmp} \le \sum_{e^{-}_{km}\in E:\, e^{-}_{km}\ge 0} z^{t(t+TT_{km})e}_{km(e-c_{km})} \cdot ECAP$	$\forall k,m \in V_h, t \in T$	(I.12)	(II.2)
$n^t_{ke} \ge \sum_{e^{-}_{km}\in (m\in V_h):\, e^{-}_{km}\ge 0} \sum_{u\in T} z^{tue}_{km(e-c_{km})} + \sum_{e^{-}_{km}\in (m\in V_h):\, e^{-}_{km}\ge 0} \sum_{u\in T} r^{tue}_{km(e-c_{km})}$	$\forall k \in V_h, t \in T,$ $e \in E$	(I.13)	(II.3)
$n^t_{ke} - \sum_{e^{-}_{km}\in (m\in V_h):\, e^{-}_{km}\ge 0} \sum_{u\in T} z^{tue}_{km(e-c_{km})} + \sum_{e+rate^{-}_{mk}\in (m\in V_h):\, e+rate^{-}_{mk}\ge 0} \sum_{u\in T} z^{ut(e+rate-c_{km})}_{mk(e+rate)} - \sum_{e^{-}_{km}\in (m\in V_h):\, e^{-}_{km}\ge 0} \sum_{u\in T} r^{tue}_{km(e-c_{km})} + \sum_{e+rate^{-}_{mk}\in (m\in V_h):\, e+rate^{-}_{mk}\ge 0} \sum_{u\in T} r^{ut(e+rate-c_{km})}_{mk(e+rate)} = n^{(t+1)}_{k(e+rate)}$	$\forall k \in V_h, t \in T,$ $e \in E : e +$ $rate < E$	(I.14)	(II.4)
$\sum_{e+rate\in E} \left(n^t_{ke} - \sum_{e^{-}_{km}\in (m\in V_h):\, e^{-}_{km}\ge 0} \sum_{u\in T} z^{tue}_{km(e-c_{km})} - \sum_{e^{-}_{km}\in (m\in V_h):\, e^{-}_{km}\ge 0} \sum_{u\in T} r^{tue}_{km(e-c_{km})} \right) = n^{(t+1)}_{kE}$	$\forall k \in V_h\ t \in T$	(I.14)	(II.5)
$\sum_{e^{-}_{mk}\in (m\in V_h):\, e^{-}_{mk}\ge 0} \sum_{u\in T} z^{ut(e-c_{km})}_{mk(e)} + \sum_{e^{-}_{mk}\in (m\in V_h):\, e^{-}_{mk}\ge 0} \sum_{u\in T} r^{ut(e-c_{km})}_{mke} = n^{(t+1)}_{ke}$	$\forall k \in V_h,$ $t \in T,$ $e \in E : e < rate$	(I.14)	(II.6)
$\sum_{(k,m,u,w,e):t\in betwn(tu)\setminus u} z^{uwe}_{km(e-c_{km})} = l_t\ (\boldsymbol{a}) \sum_{(k,m,u,w,e):t\in betwn(tu)\setminus u} r^{uwe}_{km(e-c_{km})} = g_t\ (\boldsymbol{b})$	$\forall t \in T$	(I.16)	(II.7)
$\sum_{e\in E}\sum_{k\in V_h} n^t_{ke} + l_t + g_t = v$	$\forall t \in T$	(I.17)	(II.8)
$\sum_{e\in E} z^{tue}_{km(e-c_{km})} + \sum_{e\in E} r^{tue}_{km(e-c_{km})} \le M \cdot CLOSE^{tu}_{km}$	$\forall k,m \in V_h,t,u \in T,$ $e \in E$	(I.18)	(II.9)
$y^t_{ijkmp}, s^t_{ijkmp}, r^{tue}_{kmf}, z^{tue}_{kmf}, l_t, g_t \in N$	$\forall i,j \in V_d,p \in P,$ $k,m \in V_h,t,u \in T,$ $e \in E$	(I.20)	(II.10)

Constraints (II.1) ensure, just like constraints (I.12), that the number of available eVTOLs at a UAM infrastructure point k of archetype u is not higher than the capacity of that archetype. A difference, however, is that now the number of available eVTOLs across all battery levels in E needs to be considered. The same logic applies to constraints (II.2). If demand is satisfied between a pair of vertiports from the beginning of a time interval to the end of a time interval, an eVTOL needs to be operated over all combinations of battery levels for the respective pair of vertiports. Constraints (II.3) ensure that the number of eVTOLs that leave vertiport k at the beginning of time interval t with battery level e for serving trips or relocation cannot be higher than the number of available eVTOLs at the specific vertiport with battery level e.

The typical flow conservation constraints for eVTOLs at the UAM ground infrastructure location are complex and split into three separate

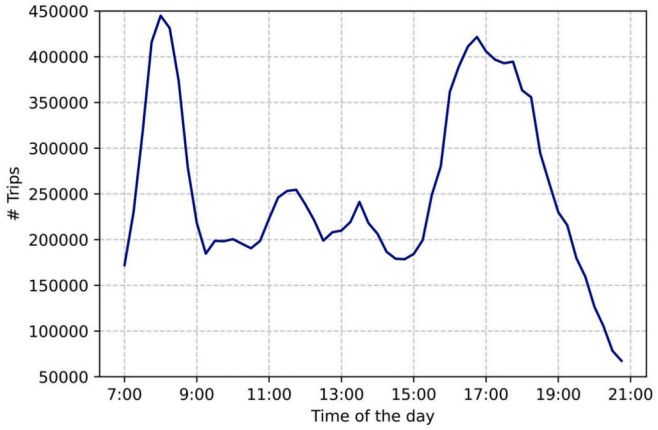

Fig. 9. Travel demand distribution over the day.

Constraints (II.4), (II.5), (II.6). All constraints ensure that the number of eVTOLs at infrastructure point k at the beginning of time interval t with battery level e is equal to the number of eVTOLs available at time $t+1$ with battery level $e + rate$ minus the eVTOLs leaving for serving trips and relocating at the beginning of time interval t and plus the eVTOLs arriving at the end of time interval t with battery level $e + rate$. Note that these constraints are written separately for cases where $e + rate < E$, E and $e < E$.

Constraints (II.7a) and (II.7b) keep track of the number of eVTOLs that are respectively serving trips or relocating over all battery level combinations at the beginning of time interval t, but started this operation before time interval t. Combining the number of eVTOLs in operation at the beginning of time interval t with the number of available eVTOLs at each vertiport at the beginning of time interval t over all battery levels give the total number of eVTOLs, as formalized in Constraints (II.8). Finally, Constraints (II.9) ensure that there are no trip serving or relocation operations over all battery level combinations during the night closure.

Fig. 7 provides an illustration of the dynamics within the space-time-battery network. An eVTOL starts with a back-and-forth trip serving operation between vertiports 4 and 5. Note that the eVTOL is able to perform this operation due to its sufficient remaining battery levels and the battery level consumption of 1 between these vertiports. Following

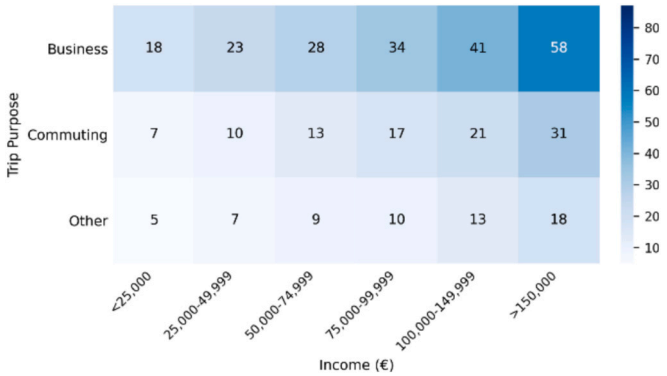

Fig. 10. Value of Time public transport users (€/hour).

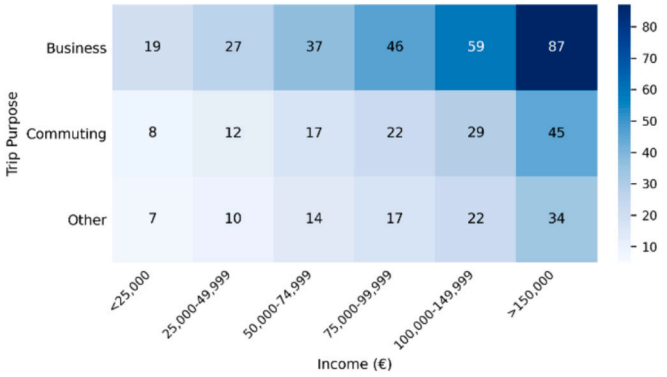

Fig. 11. Value of Time car users (€/hour).

the two flight segments, the eVTOL undergoes charging at a rate of 2 battery levels per time interval, ensuring sufficient battery life to end the service period with a relocation operation followed by a trip serving operation. Lastly, the wrap-around operation guarantees that the eVTOL commences the next service period at the same vertiport with a fully charged battery.

3.4. Problem size and preprocessing for large scale problems

In real-life instances, both models described in Eqs. (1)–(30) may result in large problem sizes, which cannot be efficiently solved. The mathematical model has seven sets of decision variables ($a_{ijkp}, b_{ijkp}, h_k, c_k, y^t_{ijkmp}, z^{tu(e)}_{km(f)}, r^{tu(e)}_{km(f)}$). The number of decision variables for sets a_{ijkp} and b_{ijkp} is $\left(V_d^2 - V_d\right) \bullet V_h$. The subtraction of V_d from V_d^2 is due to intra-zonal trips not being considered. The number of decision variables for these two sets and y^t_{ijkmp} can be significant if the number of vertiports and number of zones are high. The number of decision variables for the sets representing trip serving and relocation operations of eVTOLs is calculated using $\left(V_h^2 - V_h\right) \bullet \left(T^2 - T\right)/2 + V_h$.The multiplication term $\frac{T^2-T}{2}$is due to the absence of eVTOL movements from t2 to t1, where t2 > t1. Note the addition of V_h, representing the wrap-around operation. In the space-time-battery formulation of Model 2 an extra multiplication term is added $\frac{E^2-E}{2}$. Table 3 summarizes what was previously described.

The size of the decision variable sets can be significantly reduced by only formulating relevant decision variables. For example, it is unnecessary to have decision variables for access and egress legs from a zone i to a vertiport k that is longer than the actual trip distance. Table 4 presents a set of steps that can be taken to define only the necessary decision variables and reduce the size of the model.

Note that even after narrowing down the relocation variables in step 9 by excluding those outside the time horizon, a considerable number of them persist. With a sufficient range, a relocation may happen between a pair of UAM ground infrastructure locations. Given 52 time-intervals, 80 UAM infrastructure locations and 10 battery levels in a test case, a total of 387,788 and 2,043,311 relocation variables can be created for Model 1 and 2, respectively. It is worth noting that only less than 0.05% of these relocation arcs were ultimately selected in the model.

To narrow down the number of relocation variables even further, the approach introduced by Bekli et al. (2021) is adapted. The authors proposed to create relocation variables only around trip requests. This is substantiated by the idea that there are essentially two reasons to perform relocations in a system: to ensure availability of vehicles for trip

Table 4
Steps to define only necessary decision variables.

Steps to define relevant sets	
1:	Set the time interval size
2:	Set the time horizon in which eVTOLs can operate t_{start} and t_{end} (outside night-closure)
3:	Insert demand values OD_{ijpt}
4:	Insert travel time and costs for each population group between demand zones and vertiports, TT_{ikp} *and* TC_{ikp},between vertiports, TT_{km} and TC_{km}, and between demand zones using ground transportation, TT_{ijp} and TC_{ijp}.
5:	Insert travel times between vertiports TT_{km} discretised into time intervals TTI_{km}
6:	Inset value of time of population groups VOT_p
7:	Create set of relevant combinations of demand zones and vertiports: For each $i \in V_d, j \in V_d, p \in P \wedge i \neq j$ For each $k \in V_h, m \in V_h \wedge k \neq m$ If $\left(TT_{ijp} - \left(TT_{ikp} + TT_{jkp} + TT_{km}\right)\right) \bullet VOT_p \geq \left(TC_{ikp} + TC_{jkp} + TC_{km}\right) - TC_{ijp}$ If $OD_{ijpt} > 0$ Create potential route $r(i, j, k, m, p) \in R$
8:	Create set of relevant serving customer operations by an eVTOL: For each $r(i, j, k, m, p) \in R$ For each t $\in T$ If $OD_{ijpt} > 0$ For each $e \in FT_t \wedge e \geq t_{start} \wedge e + TTI_{km} < t_{end}$ Create potential serving customers operation $ot(k, m, t, t + TTI_{km}) \in OT$
9:	Create set of relevant relocation operations by an eVTOL: For each $k \in V_h, m \in V_h \wedge k \neq m$ For each t $\in T \wedge t \geq t_{start} \wedge t + TTI_{km} < t_{end}$ Create potential relocation operation $or(k, m, t, t + TTI_{km}) \in OR$
10	Remove duplicates from the sets OT and OR

Table 5
Objective function, solving time and average eVTOL utilization experiments.

Problem type	Criteria	Exact	Model size reduction: relocation
10 potential vertiports – 100 zones - Simple charging	Objective function (€)	525.8	488.9
	Time (s)	476	240
	Avg. eVTOL utilization	56%	54%
20 potential vertiports – 100 zones - Simple charging	Objective function (€)	1598.9	1501.0
	Time (s)	886	444
	Avg. eVTOL utilization	56%	56%
10 potential vertiports – 100 zones - Advanced charging - 5 energy levels	Objective function (€)	599.9	534.5
	Time (s)	1405	675
	Avg. eVTOL utilization	66%	64%
20 potential vertiports – 100 zones - Advanced charging - 10 energy levels	Objective function (€)	2121.3	1998.1
	Time (s)	3253	1822
	Avg. eVTOL utilization	67%	65%

Table 6
Travel time, travel cost and charging infrastructure parameters.

Parameters	Value	Source
Public transport base fare [€]	2.15	Point-to-point tickets (RATP, 2025)
PT distance fare [€/km]	0.3	Point-to-point tickets (RATP, 2025)
Car distance fare [€/km]	0.5	(Nibud, 2023)
Detour factor car	1.343	(Mennicken et al., 2023)
Detour factor walking	1.1	(Wu and Zhang, 2021)
Charging power [kW]	100–350	(Yang et al., 2021)
Average walking speed [km/h]	6	(Wu and Zhang, 2021)
Base fare UAM [€]	20	(Rath and Chow, 2022; Wu and Zhang, 2021; Ilahi et al., 2021)
UAM distance fare [€/km]	3.50, 10% and 20% discount	(Rath and Chow, 2022; Wu and Zhang, 2021; Ilahi et al., 2021)
Average cruise speed eVTOL [km/h]	75–250	(McKinsey and Company, 2025)
Detour factor UAM	Real-world routes	See appendix C

Table 7
Characteristics of considered eVTOL types.

eVTOL type	eVTOL-S	eVTOL-M	eVTOL-L
Passenger capacity [seats]	2	2 and 4	2 and 4
Battery capacity [kWh]	80	150	300
Consumption [kWh/100 km]	160	187	200
Range [km]	50	80	120
Max charging capacity [kW]	350	350	350
Acquisition cost [€/eVTOL]	594.900	1.388.100	1.983.000
Insurance cost [€/year]	26.771	62.465	89.235
Personal cost [€/km]	0,85	0,85	0,85
Energy cost [€/km]	0,15	0,31	0,38
Maintenance cost [€/km]	1,88	1,88	1,88
Daily fixed eVTOL cost [€/day]	236	551	788
Variable eVTOL cost [€/km]	2,88	3,05	3,11
Data inspired by:	Volocity, Archer Maker, eHang 216, Wisk Cora	CityAirbus, Joby S4	Lilium, Bell Nexus 4EX, Uber

serving purposes or to create availability of parking/charging spaces.

Fig. 8 shows the mechanism of this model size reduction technique. Three distinct types of relocation variables are distinguished. The first type encompasses relocation arcs inserted to facilitate the movement of eVTOLs both at the origin and destination. At the origin, they make room for incoming eVTOLs, while at the destination, they ensure availability for trip-serving purposes. These relocation arcs must begin prior to the end time of the request, constrained within a specified time window and conclude before the start of the trip request at the destination. The second type of relocation arcs is introduced after the completion of a trip, allowing an eVTOL to be assigned to another trip within a predefined time window. The final type of relocation arcs is included to facilitate trips commencing at the start of the day.

To test the effectiveness of the relocation variable reduction technique and the difference in solving time between Model 1 and Model 2, experiments were conducted with 10 and 20 potential vertiports on an Intel Xeon W-3235 CPU @ 3.30 GHz, 41 GB RAM, using Gurobi in a Windows 10 environment. Results in Table 5 show that reducing relocation variables consistently cuts solving time, though with a slight reduction in profit. A key finding is that the exact model uses relocation arcs to rebalance the system and serve more trips, even if these arcs are not directly related to trip requests. This explains the higher eVTOL utilization and profit in the exact model compared to the variable reduction model. In the reduced model, the restricted relocation set becomes binding in periods and locations with vehicle shortages, which forces some profitable demand to remain unserved despite being potentially profitable. For the same problem type, Model 2, with advanced charging, achieves a better objective function than the simpler Model 1. Model 2 allows multiple flight segments without recharging, increasing eVTOL utilization and profits, but at the cost of longer solving times. Therefore, Model 1 is more efficient for short-range eVTOLs, while Model 2 is superior for longer-range eVTOLs.

4. Île-de-France case study

The Île-de-France region, particularly the city of Paris, stands at the forefront of electric Urban Air Mobility (UAM) development. At the time of composing this paper, leading up to the 2024 Olympic Games, Paris planned to become the first European city, and potentially the first globally, to offer eVTOL services. However, in early 2024, this timeline was pushed back to at least 2025 due to prolonged certification procedures by the EU Aviation Safety Agency (EASA). Currently, EASA has only granted certification to one electric aircraft, the Pipistrel Velis Electro, which lacks vertical take-off and landing capabilities, crucial for urban operations. In the broader scope, the vision entails gradually expanding operations across the entire Île-de-France region over the next decade.

As the region is working on introducing new mobility concepts, Île-de-France and especially Paris, is facing the classic mobility problems of the major urban areas around the world, such as traffic congestion and parking shortages. According to INRIX (2022), in Paris commuters experienced in 2022 an average annual traffic delay of over 100 h, resulting in negative externalities such as economic loss and environmental pollution. The leading role of Île-de-France region in UAM development, together with the mobility problems, makes the region an interesting test bed for applying the optimization models and assessing their practical usefulness in a real-world setting.

4.1. Study data

To apply the models for the planning of a UAM system in the Íle-de-France region, first several types of data need to be obtained, namely:

- Origin-destination (OD) matrix with potential demand for UAM for each population segment.
- Travel cost and time for UAM, access and egress modes and pure ground transportation modes.
- Costs of running the UAM system.
- Candidate locations for UAM ground infrastructure.

Table 8
Model setting characteristics and GAPs for the considered scenarios.

Objective	Price	eVTOL type		# energy levels	Model	eVTOL speed [km/h]	Charging power [kW]	# scenario's	GAP in 10.000 s
Multi-objective	[Full price, 10%, 20% discount]	EVTOL-S	2-seat	1	1 -TS	125	175	21	[0.00% - 28.4%]
Profit	Full price	EVTOL-S	2-seat	1	1 -TS	[75–250]	175	7	0.00%
Profit	Full price	EVTOL-S	2-seat	1	1 -TS	125	[100–350]	11	0.00%
Profit	Full price	EVTOL-M	2-seat	8	2 -TSB	125	175	1	0.00%
Profit	Full price		4-seat	8	2 -TSB	125	175	1	0.00%
Profit	Full price	EVTOL-L	2-seat	12	2 -TSB	125	175	1	0.02%
Profit	Full price		4-seat	12	2 -TSB	125	175	1	0.02%

Table 9
Effect eVTOL designs on UAM ecosystem characteristics.

	2 -seat layout			4 -seat layout	
	eVTOL-S	eVTOL-M	eVTOL-L	eVTOL-M	eVTOL-L
Infrastructure					
Nr of vertistops	8	10	5	19	19
Nr of vertiports	0	0	0	2	1
Nr of vertihubs	0	0	0	3	1
Nr of UAM infrastructure locations	8	10	5	24	21
Fleet					
Nr of eVTOLs	22	22	12	48	36
Nr of trips served	719	900	598	2521	2212
Nr of trips served per vehicle	32.7	40.9	49.8	52.5	61.4
Nr of relocations	36	43	9	113	83
% time moving passengers	0.24	0.27	0.31	0.17	0.18
% time relocating	0.04	0.05	0.02	0.04	0.03
% time idle	0.44	0.53	0.61	0.37	0.38
% time charging	0.28	0.15	0.07	0.09	0.06
Average number of passengers per movement	1.70	1.69	1.31	3.67	3.93
Traveler characteristics					
Satisfied demand %	0.10	0.13	0.09	0.36	0.32
Average distance of UAM trip [km]	27.1	29.3	29.3	32.1	33.4
Objectives					
Profit operator [€/day]	4046	2131	683	31,031	25,213
Generalized travel cost savings [€/day]	3408	4126	2482	13,735	12,449

Fig. 12. Remaining cells knock-off criteria analysis.

For the OD-matrix, the synthetic travel demand and population pipeline, developed by Hörl and Balac (2021), has been applied to the Île-de-France region. From the pipeline, a dataset of over 14 million trips along with departure time was acquired. Analysis of the dataset revealed trip purposes categorized by occurrence, with home trips being the most prevalent (41%), followed by leisure (13%), work (13%), other (13%), shopping (11%), and education (8%). Transportation modes were segmented into four categories: walking (43%), car (33%), public transit (22%), and biking (1%). Fig. 9 presents the distribution of the travel demand over the day. Note that the time horizon of this study is between 7:00 AM and 9:00 PM with time intervals of 15 min, resulting in a total of 56 time intervals. The distribution shows that there are two peaks in the travel demand, a morning peak between 7:00 AM and 9:00 AM and an afternoon peak from 3:30 PM to 7:00 PM.

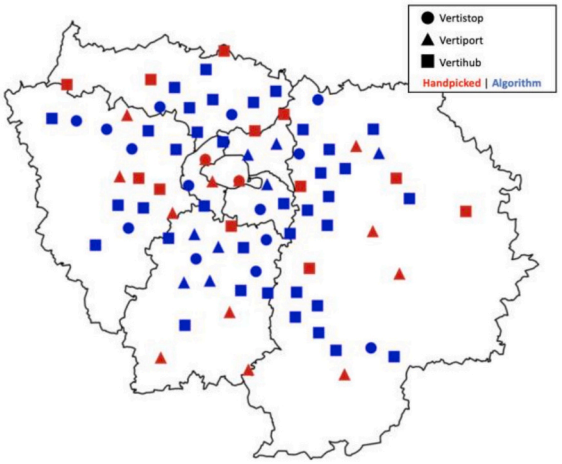

Fig. 13. Final set of candidate UAM ground infrastructure locations.

A large portion of the trips are not eligible for a UAM service and need to be filtered using the VoT criterion. Recall that a trip qualifies for UAM if it results in a net reduction in the generalized travel cost, which combines the travel cost and the travel time converted to cost using the VoT. For the VoT criterion, multiple inputs are required: the VoT for different population segments, cost and travel time parameters of UAM and the ground transportation alternatives.

Starting with the VoT, the government of France has established reference VoTs for project evaluations, transportation, and planning guidelines (Department Developement Durable, 2019). These values are differentiated across three distinct trip purposes: professional, commuting, and others (shopping, leisure, visits, care, etc.), and two modes of transportation: car and public transport. By integrating these reference parameters with income elasticities derived from Binsuwadan et al. (2023), the calculation of time values becomes possible for demographic segments with varying incomes, trip purposes, and travel modes. The resulting VoT values for different population segments are depicted in Figs. 10 and 11. In total, 36 population segments are distinguished.

For the cost and travel time parameters of pure ground transportation modes (car and public transportation), access and egress modes (walking and taxi), and UAM, a combination of outputs from the synthetic pipeline and parameters identified in the literature is applied. Travel times for car and public transportation are obtained from the synthetic pipeline, whereas cost parameters for ground transportation and UAM are taken from the literature. The remaining parameters are summarized in Table 6.

After filtering, the remaining trips form the input for the zoning algorithm. The result of the zoning algorithm is an origin-destination matrix that shows the demand between each pair of zones for each population segment, characterized by travel mode, income category, and trip purpose. Figs. A.1 and A.2 in Appendix A display the results of the zoning algorithm and the spatial distribution of income and travel demand over the zones, respectively. As expected, the potential demand for UAM is primarily concentrated in and around Paris. However, the highest average income category is found in the outer regions of Île-de-France.

This paper considers various types of eVTOL designs to accommodate the diversity of designs currently under development. Table 7 provides an overview of the eVTOL types considered, which differ primarily in range and passenger capacity. The first type, referred to as eVTOL-S, represents the near-term short-range eVTOLs with a range of up to 50 km and a maximum passenger capacity of 2 travelers. The second type, eVTOL-M, is characterized by a medium range of 80 km.

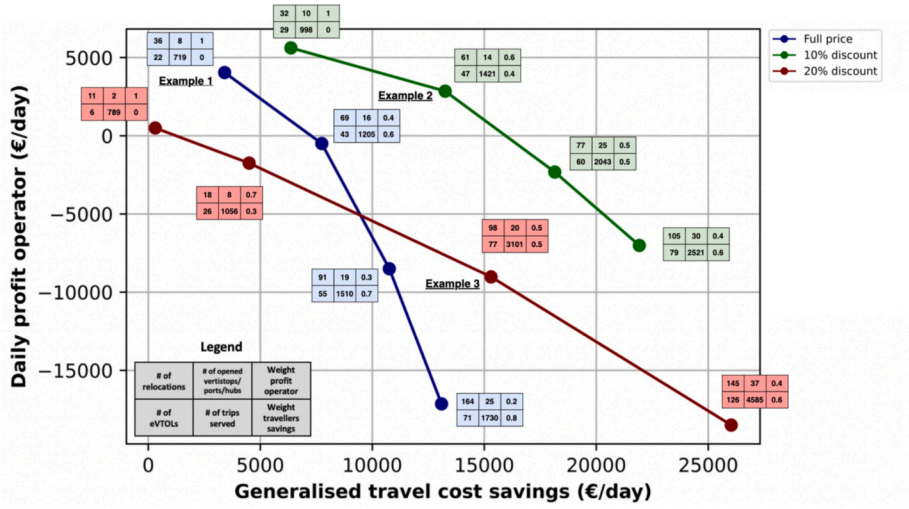

Fig. 14. Relation daily profit operator and generalized travel cost savings for different pricing scenarios.

Due to the variety of designs being developed for this range, two passenger capacity sizes are considered: 2 and 4. The final type, eVTOL-L, represents the longest range eVTOLs with a range of up to 120 km. Similarly, two passenger capacities are considered for this type: 2 and 4. For each eVTOL type, both the daily fixed eVTOL cost and the variable eVTOL cost are determined. Besides the range and passenger capacity, the maximum cruise speed and charging power vary among different eVTOL designs.

The final data requirement encompasses identifying candidate sites for UAM ground infrastructure. This study distinguishes three types of ground infrastructure, each with specific capacities and daily operating costs: vertistop (2 spots, €2137), vertiport (6 spots, €8397), and vertihub (20 spots, €42,740). These costs are based on estimates from McKinsey & Company (n.d.) and NASA (2018).

The starting point in the identification of candidate UAM ground infrastructure types is to handpick locations with a high potential in areas where eVTOLs can land and take off. Subsequently, the remaining study area is divided into a grid of cells. The potential of each cell for UAM ground infrastructure is evaluated in a GIS-analysis using knock-off criteria, as shown in Table 2.

Table B1 in Appendix B presents the outcomes of the knock-off criteria analysis, showing the number of candidate cells remaining

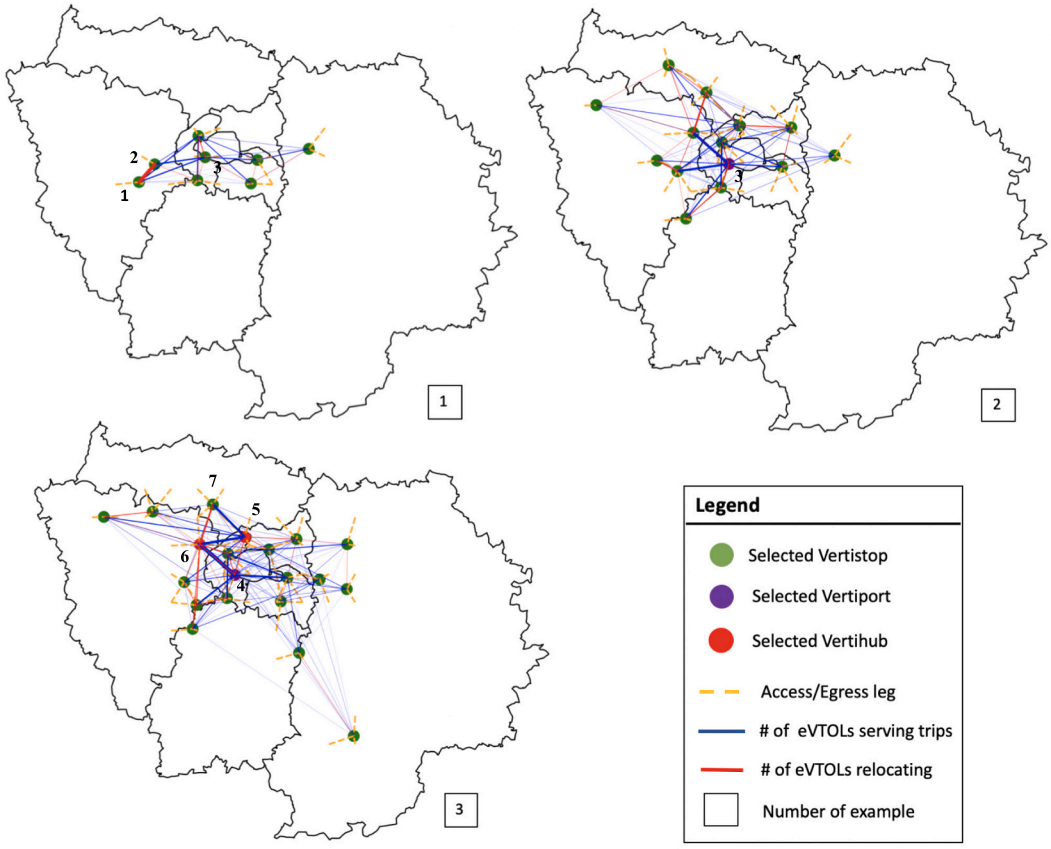

Fig. 15. UAM network structure examples.

after the application of the criteria. The starting points for the scenario analysis are two filters: airspace zoning and land use. The scenario analysis tests various rules ranging from strict to very strict. Two notable observations emerge. Firstly, the land use filter has the most impact on reducing the pool of candidate cells. Secondly, particularly in the Paris region, the influence of the strictest existing urban noise criterion is noteworthy, resulting in a limited number of remaining cells in the area.

The considerable amount of remaining candidate cells following the initial scenario analysis is primarily because extensive remote areas are not filtered using the rules stated above. Given the absence of noise data, no eligible land use categories or schools are in these remote areas. To prevent the placement of vertiports in remote areas, the applied accessibility knock-off criteria are displayed in Table B2 in Appendix B. The table highlights the significant influence of the accessibility knock-off criteria on the suitability of cells for UAM infrastructure. To conduct further analysis and identify the set of candidate UAM ground infrastructure locations, the decision is made to select the median mixed scenario with an accessibility criterion of more than 1000 activity locations. This is to ensure that cells in both dense and remote areas are not entirely excluded. Fig. 12 illustrates the remaining cells in the study area under the selected scenario. The remaining cells from the knock-off criteria analysis form the input for the candidate vertiport selection algorithm. The final output of the algorithm is a set of 85 candidate UAM ground infrastructure locations each with a maximum archetype category, shown in Fig. 13. The red and blue points represent the handpicked and resulting UAM ground infrastructure locations from the algorithm, respectively.

Travel time between selected infrastructure locations is determined by a network of paths based on existing helicopter corridors, highways, railways, and rivers to minimize noise impact and consider restricted airspaces. Fig. C1 (Appendix C) illustrates the routes.

4.2. Model solving

In this study, a comprehensive analysis is conducted across various scenarios. Table 8 provides a summary of the model settings and corresponding optimality gaps for the scenarios. Each scenario is run with the case study area divided into 167 zones and 36 population segments, and the time horizon divided into 56 time intervals, with each interval representing 15 min. The input parameters not presented in Table 8 remain constant across the scenarios.

Most scenarios are solved using the eVTOL-S type with 2 seats, within the time-space formulation of Model 1. The analysis evaluates trade-offs between daily operator profit and generalized travel cost savings across three pricing scenarios: a full price of €3.50 per passenger-kilometer, and 10% and 20% discounts, with a base fare of €20 applied uniformly. The chosen full price and base fare are based on a review of high-pricing scenarios from various sources (Ilahi et al., 2021; Fu et al., 2019; Rath and Chow, 2022). The selected values represent an average of these documented prices, ensuring our analysis is grounded in existing research.

Seven combinations of objective weights are explored, resulting in 21 distinct scenarios. Additional analyses include 7 scenarios where the eVTOL cruise speed is varied between 75 and 250 km/h (in 25 km/h increments), and 11 scenarios where the charging power is varied between 100 and 350 kW (in 25 kW increments), all using the eVTOL-S design.

The preference for Model 1 in most scenarios is motivated by three factors. First, the eVTOL-S design is anticipated to be the earliest to enter the market in the study area, making its analysis particularly relevant for decision-makers. Second, its operational characteristics, specifically charging after each flight segment, align well with the structure of Model 1. Third, Model 1 offers a more tractable formulation than the time-space-battery formulation (Model 2), especially under high-demand settings induced by lower pricing.

However, computational performance presents a notable limitation in some scenarios. Specifically, for the lowest pricing case (20% discount), an average GAP of 28.4% is observed after 10,000 s of computation time. This reduced performance is primarily due to increased travel demand, which significantly enlarges the solution space. The surge in trip requests and relocation operations leads to a combinatorial explosion in decision variables and constraints, which challenges the solver's ability to converge efficiently.

While the model remains computationally tractable for full and moderate pricing scenarios, it becomes more difficult to solve to optimality under aggressive pricing strategies. This reflects a trade-off between solution fidelity and model scalability. Therefore, although our approach captures key system dynamics and performs well across a broad range of scenarios, its application to extreme demand cases may require further model simplification, decomposition strategies, or high-performance computing resources.

4.3. Study results

This section discusses the results of the scenarios. The discussion starts in subsection 4.3.1 by providing insights into the trade-off between operator profit and generating generalized travel cost savings for travelers across various pricing scenarios. Following this, a subset of optimized networks will be explored further, focusing on their structure, size, and dynamics in subsection 4.3.2, as well as the travelers' characteristics. In subsection 4.3.3, the impact of diverse eVTOL designs in terms of passenger capacity and range on the UAM ecosystem will be outlined. Subsections 4.3.4 and 4.3.5 present an evaluation of the impact of the eVTOL cruise speed and charging power on the size of the service region, eVTOL utilization and operator's profit.

4.3.1. Trade-off profit and travel cost savings

Fig. 14 illustrates the relationship between the operator's daily profit and generalized travel cost savings across various pricing scenarios. These outcomes result from adjusting the weightings of the two objectives. Each data point is accompanied by the respective number of relocations, eVTOLs, active UAM ground infrastructure locations, and served trips. The relationship can be interpreted as an operationalization of the efficient frontier with a Pareto set of feasible outcomes for stakeholders with different priorities. Several key observations can be drawn:

I. The negative correlation between generalized travel cost savings and the daily profit of the operator across all pricing scenarios indicates that an operator should sacrifice some profit to improve the level of service for travelers, and vice versa. A larger network with more UAM ground infrastructure locations and eVTOLs results in more trips served (greater coverage and lower access/egress times) and higher revenues. However, the spatial-temporal patterns of travel demand require more relocations and/or reduce eVTOL utilization. Consequently, operating costs increase more than revenues. In other words, operators benefit from more concentrated networks with a few vertiports around demand hotspots.
II. When the UAM passenger-kilometer price is reduced by 10% compared to the full price, it becomes possible to achieve higher generalized travel cost savings for a similar daily profit. This reduction in price generates extra demand within the study area, thereby benefiting eVTOL utilization and reducing the number of relocations required. In other words, the decrease in operating margin is balanced by gains in the more efficient utilization of eVTOLs.
III. Conversely, when applying a 20% discount to the UAM passenger-kilometer price, the situation initially unfolds differently. Under this pricing scenario, the operating margin diminishes substantially. Consequently, a highly concentrated network linking demand hotspots becomes essential to mitigate

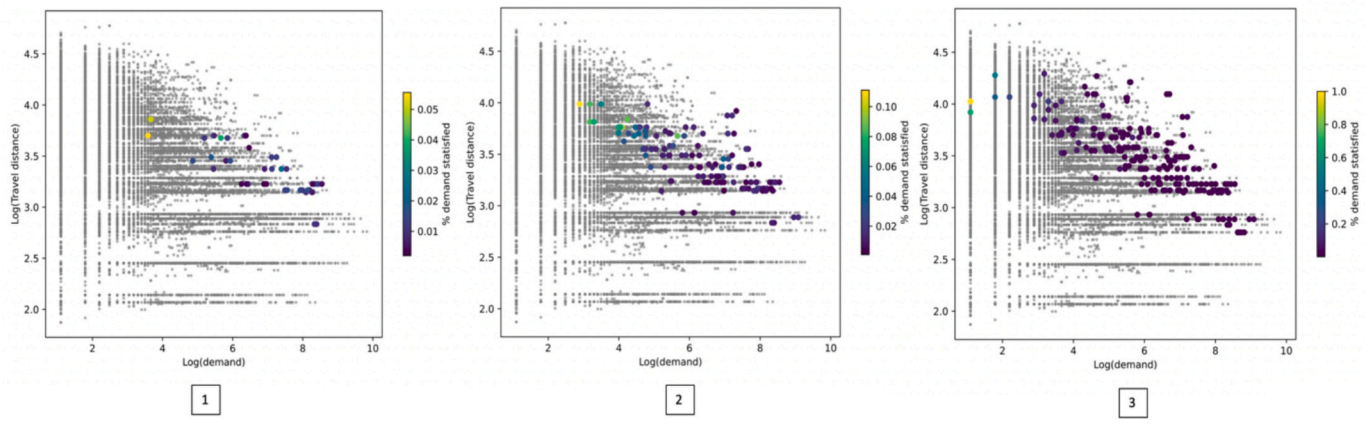

Fig. 16. Relation between demand and distance using a log scale for different examples.

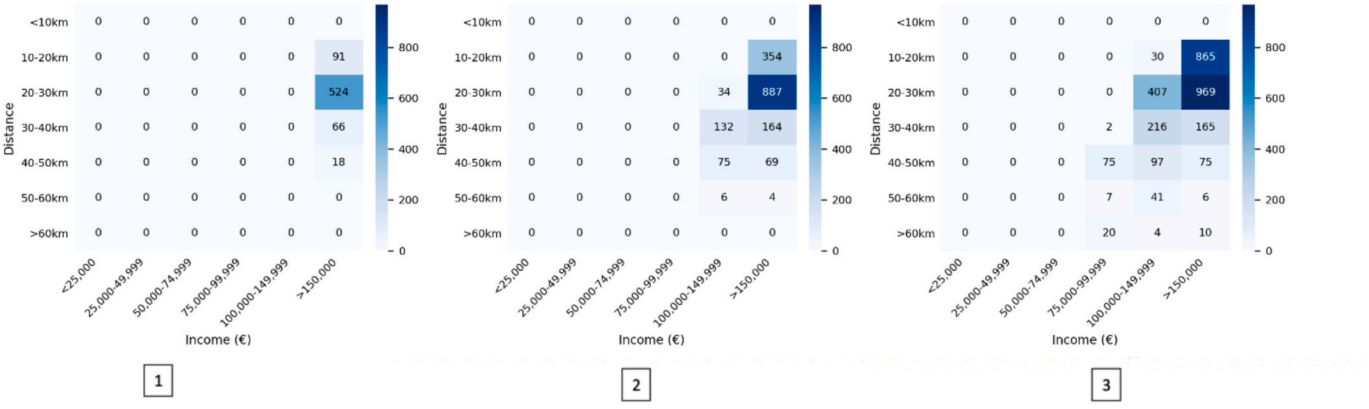

Fig. 17. Relation between income and distances for different examples.

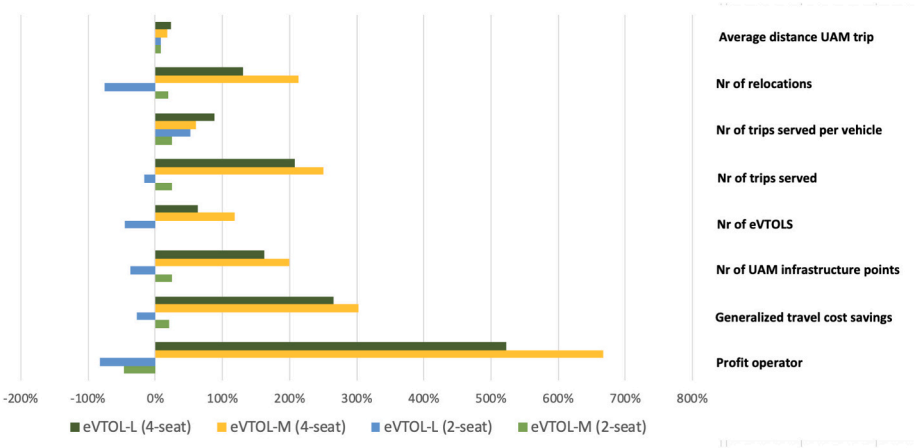

Fig. 18. Effect eVTOL design parameters on UAM ecosystem characteristics.

unnecessary relocation costs. Notably, the relationship between the operator's profit and generalized travel cost savings for the 20% discount intersects with the relation for the full price. This intersection can be attributed to two primary factors: 1) the potential influx of new users attracted by the lower price, which facilitates more efficient large-scale operations with higher vehicle utilization and fewer relocations required, and 2) existing users of UAM services under full-price scenarios now experiencing a higher consumer surplus, as reflected in the generalized travel cost savings, due to the reduced price.

IV. For future UAM operators and policymakers, it is essential to note that the marginal gain in cost savings per unit of lost profit is not constant. Expanding concentrated networks leads to greater gains in traveler benefits than expanding already dispersed networks. This implies that networks not yet saturated have more growth potential in terms of attracting new users without disproportionate cost increases.

To summarize, each point along this curve represents a different strategic balance between these objectives. From a stakeholder

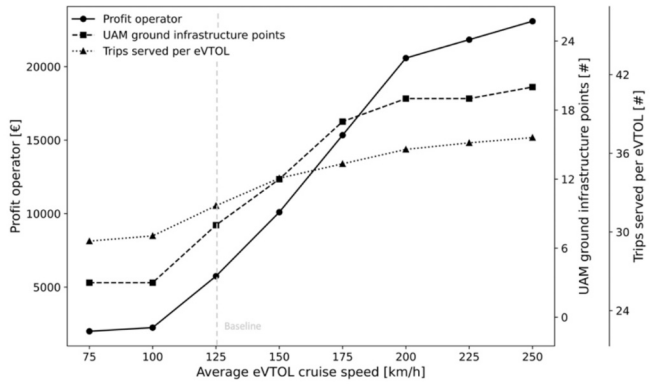

Fig. 19. Performance UAM system under different eVTOL cruise speeds.

perspective,

UAM operators may prioritize points with higher profits even if travel cost savings are lower, particularly in early deployment stages when financial sustainability is critical. Conversely, policymakers or public agencies may push toward network configurations located closer to the cost-saving end of the spectrum, as they align more with societal objectives such as accessibility and equity. This tension highlights the importance of shared governance or incentive alignment to determine an acceptable compromise along the efficient frontier.

4.3.2. Structure of UAM networks and characteristics UAM traveler

Three optimized networks are selected for further analysis to illustrate how pricing and objective weighting shape network structure and operations:

- Example 1, Full price, profit-maximizing solution: Profit weight = 1.0; generalized travel cost weight = 0.0. Included to represent the most profitable network under the full-price regime.
- Example 2, 10% discount, profit-prioritized trade-off: Profit weight = 0.6; generalized travel cost weight = 0.4. Included to compare how a modest fare reduction and an explicit profit–generalized travel cost trade-off affect a profitable network configuration.
- Example 3, 20% discount, balanced trade-off: Profit weight = 0.5; generalized travel cost weight = 0.5. Included to illustrate a relatively high-service network under the lowest pricing scenario.

The structures of the UAM networks of the three examples are presented in Fig. 15. The structure of Example 1's network, in which the operator's profit is maximized under full pricing conditions, is characterized by its interconnectivity centered around Paris. This centrality is attributed to three factors: 1) Concentrated demand in this area, primarily among higher income segments, 2) Increased travel time due to congestion effects, making UAM an attractive alternative and 3) full pricing scenario makes long-distance UAM trips relatively unattractive cost-wise compared to the current ground transportation alternatives. In the longer distance markets, congestion plays a less significant role.

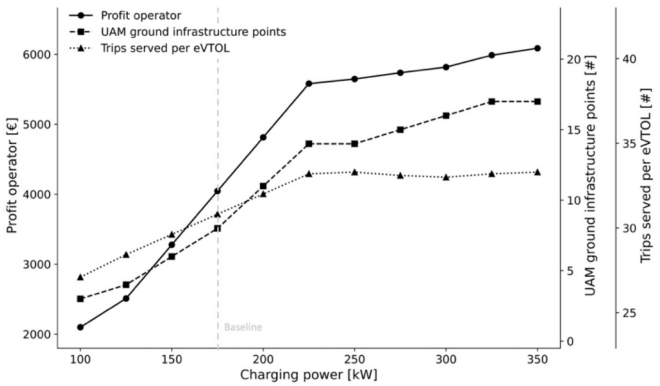

Fig. 20. Performance UAM system under different charging power levels.

In Example 1's network, two vertiports are labeled 1 and 2, each illustrating important dynamics within the model. First, it shows that not all UAM ground infrastructure locations serve the same function. Vertistop 1 primarily functions as an arrival location for travelers, whereas vertistop 2 primarily serves as a departure point for trips. Second, geographic interdependence is evident: some highly attractive areas with significant demand may remain uncovered, while less attractive areas may be served due to the presence of neighboring complementary markets. In this network, neither vertiport has the highest demand potential; however, both are selected due to the relatively low relocation cost between the locations.

The network in Example 2 expands in a nested fashion as a result of the pricing discount and associated increase in demand. While a core of interconnected infrastructure remains around central Paris, new vertiports begin to appear in residential areas, extending the reach of the network. The result is a hybrid configuration that includes both interconnected and star network structures, enabling broader coverage and improved access for users outside of the urban core.

In Example 3, the 20% price discount generates interest in UAM across a broader population, including those located further from the city center. This leads to the formation of a more dispersed network, with demand hotspots emerging in previously underserved areas. Expansion occurs primarily through the addition of the smallest UAM infrastructure type, the vertistop. As a result, the network structure becomes decentralized, targeting localized demand clusters that benefit from shorter access and egress distances.

The network also includes one vertiport (labeled as 4) and two vertihubs (labeled as 5 and 6), along with a vertistop labeled as 7, which together form a diamond-shaped core. Vertiport 4 and vertihub 5 are located in the inner region of Paris, while vertihub 6 is situated in the outer region. This structure supports trip-serving operations primarily between the inner and outer regions, while relocation operations are more common within each region. These patterns are explained by two factors: first, commuting demand is predominantly one-directional, with travelers moving toward central Paris in the morning and returning in the evening; second, intra-regional travel within the outer region is limited, and trips within the inner region are often too short to justify UAM use or are already well-served by public transit. The asymmetry of commuter flows results in imbalances in vehicle distribution, necessitating strategic relocations to high-capacity infrastructure nearby.

Comparing the locations of the opened UAM ground infrastructure locations in the three examples, it becomes clear that a ground infrastructure point opened in a (short-term) high pricing scenario is not necessarily selected in networks with 10% and 20% discounts in UAM pricing. Lower pricing scenarios create new markets, which can lead to a restructuring of the network. This restructuring is further stimulated by geographic interdependence, making the network structure easily adjustable. In addition, the results show that fleet size increases with network expansion and dispersion, rising from 22, 45, and 77 eVTOLs in Examples 1, 2, and 3, respectively. In short, these dynamics highlight the complex interaction between strategic decisions on the location and size of UAM ground infrastructure, tactical decisions on eVTOL fleet size, and operational decisions on demand pooling, routing, and repositioning of eVTOLs to meet passenger demand.

4.3.3. Demand patterns and socioeconomic characteristics

Fig. 16 presents satisfied UAM demand for all origin–destination (OD) pairs as a function of total demand and travel distance on a logarithmic scale. Grey dots indicate OD pairs not served by UAM, whereas colored dots indicate served OD pairs, with color denoting the share of trips captured by UAM for that OD pair. The analysis reveals that UAM is

generally not competitive for short-distance trips. This is primarily due to the base cost of UAM, which remains constant regardless of trip length and cannot be justified by minimal time savings over such distances. Particularly in Example 1, UAM is also less competitive on longer-distance trips. This can be attributed to two factors: first, the majority of travel demand in the study area falls within the 20 to 40-km range, where UAM provides the greatest balance of cost-effectiveness and travel time savings; and second, the full-pricing scenario renders longer-distance UAM trips financially less attractive compared to conventional ground transportation options. In Examples 2 and 3, where pricing is reduced, a higher number of longer-distance trips are served, indicating increased demand elasticity and broader spatial viability of UAM services.

Fig. 17 illustrates the relationship between income levels and trip distances across the three examples. Under the full-price scenario in Example 1, only travelers from the highest income group are willing to use UAM services, as their higher value of time makes the premium pricing more justifiable. The 10% price reduction in Example 2 expands the user base to include individuals from two income categories, demonstrating increased affordability and accessibility. In Example 3, with a 20% price reduction, UAM becomes attractive to three distinct income groups, significantly broadening the socio-economic reach of the service.

These observations reinforce the idea that pricing plays a critical role in shaping both the structure of UAM networks and the demographic profile of their users. By adjusting pricing strategies and network configurations, operators can optimize for different policy goals, whether they be profitability, equity of access, or overall service quality.

4.3.4. *Effect of eVTOL designs – Range and Passenger capacity*

Table 9 provides an overview of how different eVTOL designs impact the number of UAM infrastructure locations, fleet size, fleet operations, traveler characteristics, and objectives. Additionally, Fig. 18 depicts the relative changes each design causes to the ecosystem indicators compared to the base case design, eVTOL-S, which is a short-range eVTOL with a seating capacity of 2 passengers. Three important observations can be made based on the results. Note that these experiments are conducted under the full pricing scenario, focusing solely on profit maximization.

First, for the same seating capacity, the eVTOL-M and eVTOL-L designs yield lower profits for the operator compared to the base eVTOL-S design. This outcome can be attributed to two primary factors: 1) the high pricing scenario limits the potential demand for UAM in long-distance markets. Consequently, increasing the range does not significantly unlock new potential demand. Table 9 indicates that the average distance of a UAM trip is not substantially affected by the range. 2) Aircraft costs are not assumed constant: both the daily fixed cost and variable operating cost are specified per eVTOL type, see Table 7, and increase with eVTOL range and seating capacity. Second, the range of the eVTOL does influence the utilization rate of the vehicle if the seating capacity stays equal. Results indicate an increase in the number of trips served per day from 32.7 for the short-range eVTOL-S to 40.9 for the eVTOL-M. The increase in range allows, especially in peak periods, to do multiple flight segments and thus serve more passengers.

Finally, the seating capacity has a significant influence on the size of the UAM ecosystem. An increase in seating capacity results in the opening of more UAM ground infrastructure locations with higher capacity, more eVTOLs, more trips served, and an increase in the operator's profit and generalized travel cost savings. This outcome is driven by the revenue mechanism in the model: UAM fares are applied per passenger (not per vehicle), so revenue scales with the number of passengers carried. The underlying reason for this is relatively simple. The increase in seating capacity, therefore, improves the operating margin, despite the higher fixed and operating costs associated with higher-capacity eVTOLs.

4.3.5. *Effect of eVTOL designs – Cruise speed*

The impact of eVTOL cruise speed on key UAM system indicators is evaluated by varying the eVTOL's speed from a baseline of 125 km/h. Fig. 19 displays the resulting operator profit, number of UAM ground infrastructure locations, and fleet utilization measured by the number of trips served per eVTOL.

The findings indicate a general trend of increasing operator profit as cruise speed improves. Faster eVTOL speeds enhance the appeal of UAM services both directly and indirectly. Directly, higher speeds reduce travel time compared to ground-based alternatives, thereby stimulating demand. Indirectly, increased speed improves vehicle utilization by reducing travel times and expanding the feasible service area. This higher utilization allows fixed eVTOL costs to be spread across more trips, improving operating margins and justifying the expansion of the ground infrastructure network. Improved network coverage, in turn, reduces access and egress times, further boosting UAM demand and, consequently, operator profit.

However, the relationship between cruise speed and profit is not linear. Increasing cruise speed from 75 km/h to 100 km/h yields only modest gains in profitability. In this range, travel time savings remain insufficient to significantly shift demand from ground transportation. Similarly, when cruise speeds exceed 200 km/h, the marginal gains in profit diminish. At these speeds, the potential market becomes saturated, and additional revenue is offset by increased costs associated with fleet operations, demand imbalances, and the fixed costs of expanding infrastructure

These findings suggest that regulatory frameworks and design standards for future UAM systems in the case study region should prioritize eVTOL speeds of up to 200 km/h. Speeds beyond this threshold offer limited additional benefit while potentially incurring higher costs.

4.3.6. *Effect of charging infrastructure – Charging rate*

To investigate the potential effects of utilizing faster chargers, the charging power is varied from the baseline charging power set at 175 kW (Yang et al., 2021). The resulting operator's profit, number of opened UAM ground infrastructure locations and eVTOL fleet utilization in terms of the number of trips served per eVTOL are plotted in Fig. 20

In this study, charging speeds are inversely proportional to the charging power. The expectation is, therefore, that applying faster chargers directly reduces the downtime due to charging and thus improves the eVTOL utilization. Not surprisingly, Fig. 20 shows that faster charging technologies result in a higher number of trips served per eVTOL. The improved eVTOL utilization also benefits the size of the service region. The same fixed eVTOL costs can be spread over more trips, resulting in a higher operating margin and an increase in the number of opened UAM ground infrastructure locations.

While the general trend indicates that operator profit rises with improved charging power, stability in eVTOL utilization and service region size is observed once the charging power reaches 225 kW and above. This phenomenon can be explained by two factors. Firstly, demand saturation at existing UAM ground infrastructure locations, alongside demand imbalances and fixed costs associated with opening new ground infrastructure locations, hinders further improvements in operator profit. Secondly, the scenarios are run for the full pricing scenario. As mentioned before, the full pricing scenario results in primarily short-distance markets for UAM. As a result of the short-distance air taxi flights, improvements in charging power become negligible from a certain threshold.

In practice, the deployment of high-powered charging infrastructure is more expensive and comes at the expense of a shortened battery life in the eVTOLs. Although the additional cost of the charging infrastructure and the deterioration of the eVTOL battery life are not included in the objective function of the optimization models, the findings suggest that it is sufficient to deploy medium-speed chargers, as potential gains from further improvements in the charging power are limited.

Compared to the eVTOL cruise speed, the charging power has less of

an impact on the key indicators of the UAM system. The reason lies in the demand-supply interaction. As mentioned in the previous subsection, the increase in eVTOL speed improves the attractiveness of the UAM both directly and indirectly. However, the charging power only has an indirect influence on the UAM system attractiveness via the changes in the eVTOL utilization.

5. Conclusions and future work

The proposed framework in this paper closes a gap in existing literature for a multi-objective model that simultaneously decides on strategic decisions regarding vertiport location, size and number, tactical decisions on fleet size and operational decisions spanning eVTOL routing, repositioning and charging, while capturing the interaction of these decisions with passenger demand. The framework consists of a knock-off criteria analysis model for the identification of a realistic set of candidate locations for vertiports, two IP models for interaction between the strategic, tactical, and operational decision levels, and pre-processing techniques to generate near-optimal solutions for real-world instances. The framework is tested in a large-scale real-world setting in the Ile-de-France region.

The model provides decision-makers with ample opportunities to conduct sensitivity analysis on key parameters, particularly beneficial for determining challenging-to-establish cost values like the daily operating cost of UAM ground infrastructure. Additionally, its multi-objective framework enables decision-makers to assess the trade-offs between operator profitability and user service levels from a public perspective, a critical aspect given the regulatory hurdles associated with UAM system planning.

An important conclusion of the analysis is that, in practice, the UAM system is likely to be used primarily by an affluent segment of the population. This aligns with expectations but confirms that the system will cater to a small number of wealthy individuals, given the high costs associated with UAM travel.

An example of a result that is generalizable is the negative correlation observed between the generalized travel cost savings and the daily profit of the operator, for all pricing scenarios. A larger network with larger-scale operations, more UAM ground infrastructure locations, and eVTOLs results in more trips served and higher revenues. However, spatial-temporal one-way patterns of travel demand found in most urban regions can be such that more relocations are needed and/or reduced eVTOL utilization. Operators thus benefit from more concentrated networks with a few vertiports around demand hotspots.

Another generalizable result is the principle of geographic interdependence in UAM network structures. This concept suggests that while some highly attractive areas with significant demand may not be covered, less attractive areas may be served due to the presence of neighboring complementary markets. Notably, UAM ground infrastructure locations selected under a (short-term) high-pricing scenario are not necessarily chosen under lower-pricing scenarios. The latter can activate new demand markets, often leading to a restructuring of the network. As a result, geographic interdependence introduces considerable variability into the network configuration.

Furthermore, the results indicate that the marginal profit impact of increasing eVTOL cruise speed is non-linear. At very low speeds, increasing speed improves profitability up to a practical range of roughly 100–200 km/h, where UAM becomes sufficiently time-competitive to attract demand. Beyond this range, additional speed increases yield only marginal profit gains because the incremental demand response is limited and is offset by higher fixed costs associated with expanding the ground infrastructure network and by additional relocation costs due to demand imbalances.

Nevertheless, the model relies on simplifying assumptions that may limit the external validity of the results in real-world applications. First, the model assumes a homogeneous fleet with fixed eVTOL characteristics, whereas in practice, a variety of vehicle types will likely coexist, each with different cost structures and operational capabilities. Second, the demand model is limited to cost and travel time sensitivity and does not capture behavioral aspects such as risk aversion, willingness to share rides, or perceptions of safety, which will heavily influence UAM adoption. While necessary for tractability, these simplifications should be acknowledged when interpreting the results.

Furthermore, the current model operates under deterministic assumptions. While this allows for clear comparison of alternative system configurations, it limits the ability to capture uncertainty in factors like demand fluctuations, adverse weather, or disruptions to routing. This is particularly relevant when decisions at one level, such as vertiport placement, may influence the broader context and behavior in complex ways. Including a discussion of such limitations is important when applying the model to policy or investment decisions.

In addition to theoretical contributions, the framework offers several practical insights for UAM stakeholders. Planners can use the model to identify cost-efficient network designs, prioritize investments in high-impact areas, and evaluate pricing strategies that balance public access with operational viability. The geographic interdependence insight is particularly useful for understanding where regulatory or public support may be needed to ensure equitable coverage. Furthermore, the model can support long-term planning under different regulatory or market scenarios by stress-testing the system against varying user behavior or cost conditions.

Future work should focus on refining the model's realism without compromising scalability. Incorporating heterogeneity in the fleet, such as multiple vehicle types with different capacities and ranges, would better reflect likely deployment scenarios. The demand model could be expanded using stated preference data or calibrated behavioral models to better capture user adoption. Additionally, embedding stochastic elements would allow for more robust network design under uncertainty. Methodologically, improvements in solving efficiency, through heuristics, decomposition methods, or problem-specific relaxations, are needed to tackle increasingly complex settings.

In summary, the proposed framework closes a gap in UAM planning models by capturing multi-level decisions in an integrated manner. It offers a platform for both theoretical analysis and applied decision support. With further refinement, it has strong potential to support the implementation of efficient, realistic, and adaptable UAM networks.

CRediT authorship contribution statement

Sam Randeraad: Writing – review & editing, Writing – original draft, Visualization, Validation, Software, Project administration, Methodology, Formal analysis, Data curation, Conceptualization. **Marta Ribeiro:** Writing – review & editing, Validation, Supervision, Methodology, Conceptualization. **Jan Anne Annema:** Writing – review & editing, Validation, Supervision, Methodology, Conceptualization. **Gonçalo Homem de Almeida Correia:** Writing – review & editing, Validation, Supervision, Methodology, Conceptualization.

Appendix A. Spatial distribution of income and demand Ile-de-France region

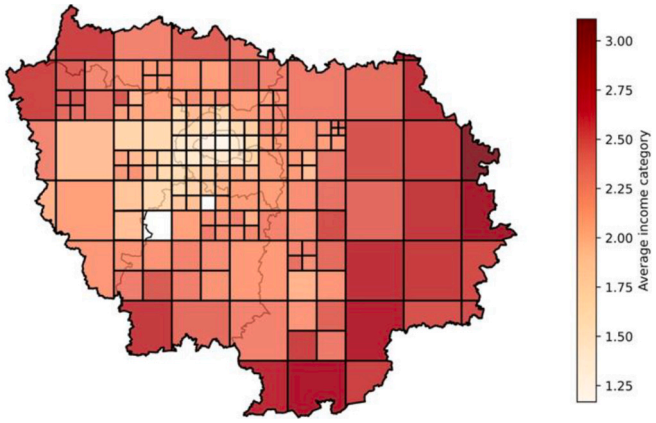

Fig. A.1. Spatial distribution of income Ile-de-France region.

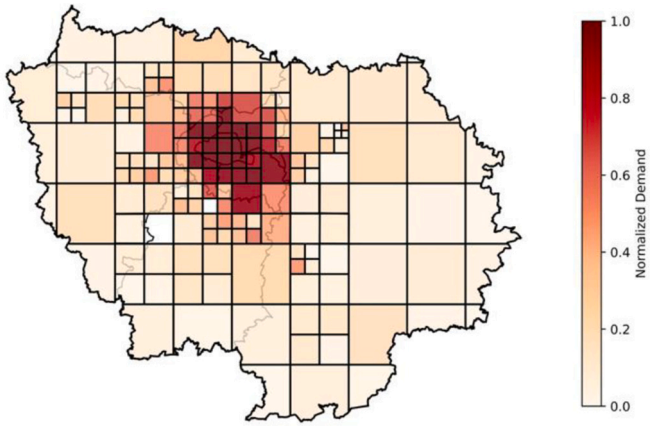

Fig. A.2. Spatial distribution potential UAM demand Ile-de-France region.

Appendix B. Knock-off criteria analysis

Table B1
Knock-off criteria results.

Rules	Description	# Candidate cells	% Base
No knock-off criteria	All available cells	1,211,716	100,0%
PA	Prohibited airspace filter	1,102,307	91,0%
PA + LU	(Airspace and land use filter) = **Base**	790,818	65,3%
PA + LU + N1	Base and existing urban noise $\geq$ 60 dB	739,847	61,1%
PA + LU + N2	Base and existing urban noise $\geq$ 70 dB	713,849	58,9%
PA + LU + N3	Base and existing urban noise $\geq$ 80 dB	700,055	57,8%
PA + LU + BS1 + BH1	Base and buffer $\geq$ 500 m	777,658	64,2%
PA + LU + BS2 + BH2	Base and buffer $\geq$ 750 m	759,585	62,7%
PA + LU + BS3 + BH3	Base and buffer $\geq$ 1000 m	735,791	60,7%
PA + LU + N1 + BS1 + BH1	Best mixed scenario	728,499	60,1%
PA + LU + N2 + BS2 + BH2	Median mixed scenario	693,460	57,2%
PA + LU + N3 + BS3 + BH3	Strictest mixed scenario	669,330	55,2%

Table B2
Knock-off accessibility results.

Rules	Description	PA x LU x N1 x BS1 x BH1 (Best)	PA x LU x N2 x BS2 x BH2 (Median)	PA x LU x N1 x BS1 x BH1 (Strictest)
A1	> 500 activity locations	19,0%	16,5%	14,9%
A2	> 1000 activity locations	9,0%	6,9%	5,7%
A3	> 1500 activity locations	5,7%	3,9%	2,9%

Appendix C. Network of paths between UAM ground infrastructure locations

Fig. C1. Network of paths between UAM ground infrastructure locations.

Data availability

Data will be made available on request.

References

Alves, C.J.P., Silva, E.J., Müller, C., Borille, G.M.R., Guterres, M.X., Arraut, E.M., Peres, M.S., Santos, R.J., 2020. Towards an objective decision-making framework for regional airport site selection. J. Air Transp. Manag. 89, 101888. https://doi.org/10.1016/j.jairtraman.2020.101888.

Archer Aviation, 2025. Archer Unveils Vision for New York Air Taxi Network, Including Routes between Manhattan and Nearby Airports in Partnership with United Airlines. https://investors.archer.com/news/news-details/2025/Archer-Unveils-Vision-for-New-York-Air-Taxi-Network-Including-Routes-Between-Manhattan-and-Nearby-Airports-in-Partnership-with-United-Airlines/default.aspx.

Bekli, S., Boyaci, B., Zografos, K.G., 2021. Enhancing the performance of one-way electric carsharing systems through the optimum deployment of fast chargers. Transp. Res. B 152, 118–139. https://doi.org/10.1016/j.trb.2021.08.001.

Binsuwadan, J., Wardman, M., de Jong, G., Batley, R., Wheat, P., 2023. The income elasticity of the value of travel time savings: a meta-analysis. Transp. Policy 136, 126–136. https://doi.org/10.1016/j.tranpol.2023.03.013.

Blad, K., Correia, G.H.A., Nes, R., Annema, J.A., 2022. A methodology to determine suitable locations for regional shared mobility hubs. Case Stud. Transp. Policy 10 (3), 1904–1916. https://doi.org/10.1016/j.cstp.2022.08.005.

Bluenest, 2023. Whitepaper: Shaping the Future of Advanced Air Mobility with Vertiports Infrastructure. https://www.bluenest.io/whitepaperform.

Boo, J., Lee, S.Y., Song, B.D., 2023. The UAM service network: multi-objective and multi-period design for UAM airports. Asia Pac. J. Mark. Logist. 35 (12), 3091–3116. https://doi.org/10.1108/APJML-03-2022-0257.

Boyaci, B., Zografos, K.G., Geroliminis, N., 2015. An optimization framework for the development of efficient one-way car-sharing systems. Eur. J. Oper. Res. 240 (3), 718–733. https://doi.org/10.1016/j.ejor.2014.07.020.

Centers for Disease Control and Prevention, 2019. What noises cause hearing loss? https://www.cdc.gov/hearing-loss/causes/?CDC_AAref_Val=https://www.cdc.gov/nceh/hearing_loss/what_noises_cause_hearing_loss.html.

Correia, G.H.A., Antunes, A.P., 2012. Optimization approach to depot location and trip selection in one-way carsharing systems. Transp. Res. Part E Logist. Transp. Rev. 48 (1), 233–247. https://doi.org/10.1016/j.tre.2011.06.003.

Department Developement Durable, 2019. Valuers Recommandees Pour le Calcul Socio-Economique. https://www.ecologie.gouv.fr/sites/default/files/V.3.pdf.

EASA, 2022. Prototype Technical Design Specifications for Vertiports. EASA Europe. https://www.easa.europa.eu/en/document-library/general-publications/prototype-technical-design-specifications-vertiports.

EvE, 2022. Concept of Operations for Sustainable Urban Air Mobility in Rio De Janeiro. https://eveairmobility.com/a-collaboration-led-by-eve-publishes-concept-of-operations-for-urban-air-mobility-in-rio-de-janeiro/.

Fadhil, D.N., 2018. A GIS-Based Analysis for Selecting Ground Infrastructure Locations for Urban Air Mobility. Master's Thesis. Technical University Munich. https://www.mos.ed.tum.de/fileadmin/w00ccp/tb/theses/fadhil_2018.pdf.

Farahani, R.Z., SteadieSeifi, M., Asgari, N., 2010. Multiple criteria facility location problems: a survey. Appl. Math. Model. 7, 1689–1709. https://doi.org/10.1016/j.apm.2009.10.005.

Fu, M., Rothfeld, R., Antoniou, C., 2019. Exploring preferences for transportation modes in an urban air mobility environment: Munich case study. Transp. Res. Rec. 2673 (10), 422–427. https://doi.org/10.1177/0361198119843858.

Garrow, L.A., German, B.J., Leonard, C.E., 2021. Urban air mobility: a comprehensive review and comparative analysis with autonomous and electric ground transportation for informing future research. Transp. Res. Part C: Emerg. Technol. 132, 103377. https://doi.org/10.1016/j.trc.2021.103377.

Hörl, S., Balac, M., 2021. Synthetic population and travel demand for Paris and Île-de-France based on open and publicly available data. Transp. Res. Part C: Emerg. Technol. 130, 103291. https://doi.org/10.1016/j.trc.2021.103291.

Husemann, M., Kirste, A., Stumpf, E., 2023. Analysis of cost-efficient urban air mobility systems: optimization of operational and configurational fleet decisions. Eur. J. Oper. Res. https://doi.org/10.1016/j.ejor.2023.04.040.

Husemann, M., Lahrs, L., Stumpf, E., 2023. The impact of dispatching logic on the efficiency of urban air mobility operations. J. Air Transp. Manag. 108, 102372. https://doi.org/10.1016/j.jairtraman.2023.102372.

Ikotun, A.M., Ezugwu, A.E., Abualigah, L., Abuhaija, B., Heming, J., 2023. K-means clustering algorithms: a comprehensive review, variants analysis, and advances in the era of big data. Inf. Sci. 622, 178–210. https://doi.org/10.1016/j.ins.2022.11.139.

Ilahi, A., Belgiawan, P.F., Balac, M., Axhausen, K.W., 2021. Understanding travel and mode choice with emerging modes; a pooled SP and RP model in greater Jakarta, Inodensia. Transp. Res. A Policy Pract. 150, 398–422. https://doi.org/10.1016/j.tra.2021.06.023.

INRIX, 2022. Global Traffic Scorecard 2022. https://inrix.com/scorecard/.

Junyent, I.A., Casanovas, M.M., Roukouni, A., Sanz, J.M., Blanch, E.R., Correia, G.H.A., 2024. Planning shared mobility hubs in European cities: a methodological framework using MCDA and GIS applied to Barcelona. Sustain. Cities Soc. 106, 105377. https://doi.org/10.1016/j.scs.2024.105377.

Kabak, M., Erbas, M., Cetinkaya, C., Özceylan, E., 2018. A GIS-based MCDM approach for the evaluation of bike-share stations. J. Clean. Prod. 201, 49–60. https://doi.org/10.1016/j.jclepro.2018.08.033.

Kohlman, L.W., Patterson, M.D., Raabe, B.E., 2019. Urban air mobility network and vehicle type – modelling and assessment. https://ntrs.nasa.gov/api/citations/20190001282/downloads/20190001282.pdf.

Li, X., 2023. Repurposing existing infrastructure for urban air mobility: a scenario analysis in Southern California. Drones 7 (1), 37. https://doi.org/10.3390/drones7010037.

Li, S., Egorov, M., Kochenderfer, M.J., 2020. Analyses of Fleet management and infrastructure constraints in on-demand urban air mobility operations. AIAA Aviation Forum 2020, 1–19. https://doi.org/10.2514/6.2020-2907.

Lim, E., Hwang, H., 2019. The selection of Vertiport location for on-demand mobility and its application to Seoul metro area. Int. J. Aeronaut. Space Sci. 20, 260–272. https://doi.org/10.1007/s42405-018-0117-0.

Lu, M., Perez, E.J., Mason, K., Li, M.Z., 2025. A hierarchical spatial and temporal optimisation of the air-high speed rail intermodal network. J. Transp. Geogr. 123, 104085. https://doi.org/10.1016/j.jtrangeo.2024.104085.

McKinsey & Company, 2025. To Take off, Flying Vehicles First Need Places to Land. https://www.mckinsey.com/industries/automotive-and-assembly/our-insights/to-take-off-flying-vehicles-first-need-places-to-land.

Mennicken, E., Lemoy, R., Caruso, G., 2023. Road network distances and detours in Europe: radial profiles and city size effects. Environ. Plann. B Urban Anal. City Sci. 51 (1). https://doi.org/10.1177/23998083231168.

Michelmann, J., Straubinger, A., Becker, A., Al Haddad, C., Plötner, K.O., Hornung, M., 2020. Urban air mobility 2030+: pathways for UAM – a scenario-based analysis. In: Proceedings of the Deutscher Luft- und Raumfahrtkongress (DLRK), 2020. https://mediatum.ub.tum.de/doc/1576768/1576768.pdf.

Mishra, S., Sahu, P.K., Sarkar, A.K., Mehran, B., Sharma, S., 2019. Geo-spatial site suitability analysis for development of health care units in rural India: effects on habitation accessibility, facility utilization and zonal equity in facility distribution. J. Transp. Geogr. 78, 135–149. https://doi.org/10.1016/j.jtrangeo.2019.05.017.

Moeckel, R., Donnely, R., 2015. Gradual rasterization: redefining spatial resolution in transport modelling. Environ. Plann. B. Plann. Des. 2015 (42), 888–903. https://doi.org/10.1068/b130199p.

NASA, 2018. Urban Air Mobility (UAM) Market Study. https://ntrs.nasa.gov/api/citations/20190001472/downloads/20190001472.pdf.

Nibud, 2023. Autokosten. https://www.nibud.nl/onderwerpen/uitgaven/autokosten/.

Niklab, M., Dzikus, N., Swaid, M., Berling, J., Lührs, B., Lau, A., Terekhov, I., Gollnick, V., 2020. A collaborative approach for an integrated modeling of urban air transportation systems. Aerospace 7 (5), 50. https://doi.org/10.3390/aerospace7050050.

Patel, S.R., Gunady, N.I., Rao, A.K., Wright, E.C., DeLaurentis, D., 2022. Modeling energy infrastructure of future electric urban air mobility operations. In: 17th Annual System of Systems Engineering Conference (SOSE), 2022, pp. 382–387. https://doi.org/10.1109/SOSE55472.2022.9812635.

Pons-Prats, J., Zivojinovic, T., Kuljanin, J., 2022. On the understanding of the current status of urban air mobility development and its future prospects: commuting in a flying vehicle as a new paradigm. Transp. Res. Part E Logist. Transp. Rev. 166, 102868. https://doi.org/10.1016/j.tre.2022.102868.

Rajendran, S., Shulman, J., 2020. Study of emerging air taxi network operation using discrete-event systems simulation approach. J. Air Transp. Manag. 87, 101875. https://doi.org/10.1016/j.jairtraman.2020.101857.

Rajendran, S., Srinivas, S., 2020. Air taxi service for urban mobility: a critical review of recent developments, future challenges, and opportunities. Transp. Res. Part E Logist. Transp. Rev. 143, 102090. https://doi.org/10.1016/j.tre.2020.102090.

Rajendran, S., Zack, J., 2019. Insights on strategic air taxi network infrastructure locations using an iterative constrained clustering approach. Transp. Res. Part E Logist. Transp. Rev. 128, 470–505. https://doi.org/10.1016/j.tre.2019.06.003.

Rath, S., Chow, J.Y.J., 2022. Air taxi skyport location problem with single-allocation choice-constrained elastic demand for airport access. J. Air Transp. Manag. 105, 102294. https://doi.org/10.1016/j.jairtraman.2022.102294.

RATP, 2025. Travel Passes and Prices. https://www.ratp.fr/en/titres-et-tarifs.

Rediske, G., Burin, H.P., Rigo, P.D., Rosa, C.B., Michels, L., Siluk, J.C.M., 2021. Wind power plant site selection: a systematic review. Renew. Sust. Energ. Rev. 148, 111293. https://doi.org/10.1016/j.rser.2021.111293.

Rimjha, M., Holte, S., Trani, A., Hinze, N., 2021. Commuter demand estimation and feasibility assessment for urban air mobility in northern California. Transp. Res. A Policy Pract. 148, 506–524. https://doi.org/10.1016/j.tra.2021.03.020.

Rothfeld, R.L., Balac, M., Ploetner, K.O., Antoniou, C., 2018. Agent-based simulation of urban air mobility. In: 2018 Modeling and Simulation Technologies Conference. American Institute of Aeronautics and Astronautics. https://doi.org/10.2514/6.2018-3891.

Santos, G.G.D., Birolini, S., Correia, G.H.A., 2023. A space–time-energy flow-based integer programming model to design and operate a regional shared automated electric vehicle (SAEV) system and corresponding charging network. Transp. Res. Part C. Emerg. Technol. 147, 103997. https://doi.org/10.1016/j.trc.2022.103997.

Schweiger, K., Preis, L., 2022. Urban air mobility: systematic review of scientific publications and regulations for Vertiport design and operations. Drones 6 (7), 179. https://doi.org/10.3390/drones6070179.

Shihab, S.A.M., Wei, P., Shi, J., Yu, N., 2020. Optimal eVTOL Fleet dispatch for urban air mobility and power grid services. AIAA Aviation Forum 2020, 1–18. https://doi.org/10.2514/6.2020-2906.

Shon, H., Lee, J., 2025. An optimization framework for urban air mobility (UAM) planning and operations. J. Air Transp. Manag. 124, 102720. https://doi.org/10.1016/j.jairtraman.2024.102720.

Sinha, A.A., Rajendran, S., 2023. Study on facility location of air taxi skyports using a prescriptive analytics approach. Transp. Res. Interdiscipl. Perspect. 18, 100761. https://doi.org/10.1016/j.trip.2023.100761.

SMG Consulting, 2025. Advanced Air Mobility Insights – A Complex Ecosystem. https://aamrealityindex.com/.

Staubinger, A., Rothfeld, R., Shamiyeh, M., Bütcher, K., Kaiser, J., Plötner, K.O., 2020. An overview of current research and developments in urban air mobility – setting the scene for UAM introduction. J. Air Transp. Manag. 87, 101852. https://doi.org/10.1016/j.jairtraman.2020.101852.

Vázquez, M.H., 2021. Vertiport Sizing and Layout Planning through Integer Programming in the Context of Urban Air Mobility. Master's Thesis. Technical University Munich. https://mediatum.ub.tum.de/doc/1624149/document.pdf.

Wang, K., Jacquillat, A., Vaze, V., 2022. Vertiport planning for urban aerial mobility: an adaptive discretization approach. Manuf. Serv. Oper. Manag. 24 (6), 3215–3235. https://doi.org/10.1287/msom.2022.1148.

Willey, L.C., Salmon, J.L., 2021. A method for urban air mobility network design using hub location and subgraph isomorphism. Transp. Res. Part C: Emerg. Technol. 125, 102997. https://doi.org/10.1016/j.trc.2021.102997.

Wu, Z., Zhang, Y., 2021. Integrated network design and demand forecast for on-demand urban air mobility. Engineering 7 (4), 473–487. https://doi.org/10.1016/j.eng.2020.11.007.

Yang, X., Liu, T., Ge, S., Rountree, E., Wang, C., 2021. Challenges and key requirements of batteries for electric vertical takeoff and landing aircraft. Joule 5 (7), 1644–1659. https://doi.org/10.1016/j.joule.2021.05.001.